Ancient TL

www.ancienttl.org · ISSN: 2693-0935

Issue 21(1) - June 2003
https://doi.org/10.26034/la.atl.v21.i1

This issue is published under a Creative Commons Attribution 4.0 International (CC BY):
https://creativecommons.org/licenses/by/4.0

© Ancient TL, 2003

Imaging and measurement of red-infrared stimulated luminescence (R-IRSL) from feldspar samples

Tetsuo Hashimoto*, Hayato Usuda, Naoki Mitamura*, and Takashi Yawata****
*Department of Chemistry, Faculty of Science, and **Graduate School of Science and Technology, Niigata University, Ikarashi-ninocho, Niigata, 950-2181, Japan

(Received, 6 January 2003 ; in final form 3 March 2003)

***Abstract**: When the infrared light was illuminated on granites and feldspar slices irradiated with X-rays, luminescence color images (abbreviated to IRSLCI) showed three color patterns, separable into intense yellow, red and faint violet portions. The yellow and faint violet parts were assignable to plagioclase and potassium feldspars and quartz constituent, respectively. The red color parts appeared on both potassium and albite feldspars. From spectrometry of the IRSL, two main emission peaks in the middle wavelength region, consisting of 550 nm (yellow) and 580 nm (orange), were revealed besides intense emission both in wavelengths shorter than 450 nm (violet region) and in wavelengths longer than 600 nm (red region) on every feldspar sample. The red IRSL (R-IRSL) of as-received feldspars was significantly enhanced after annealing treatment in oxidative conditions, rather than in reductive annealing conditions for 3hrs at 900^{o}C. The dose response of R-IRSL offered slower saturation of microcline in comparison with rapid saturation tendency of albite. The results are suggestive of a preferable application of R-IRSL to dating of burnt archaeological materials.*

Introduction

Hütt et al., (1988) have initially reported infrared-stimulated luminescence (IRSL) phenomena for most feldspar samples. When they shone infrared light in the range of 800-900nm on radiation-exposed feldspars, strong IRSL has been observed in visible-light wavelengths. Three kinds of broad luminescence peaks, consisting of strongest 300nm, 390nm in violet regions, and 550nm peaks in yellow-green, have been reported for the IRSL of a low-K albite sample stimulated with light emitting diode (LED) of 880nm emission peak from diode arrays (Clarke and Rendell, 1997). Krbetschek et al. (1997) have reviewed a number of IRSL-emission spectra from feldspars of differing origin and mixtures of various kinds of feldspar.

Recently, the authors have obtained, for the first time, color images of infrared stimulated luminescence (IRSL) for some granite slices, in addition to thermoluminescence color images (TLCI), afterglow color images (AGCI), photo-induced phosphorescence (PIP), color center images (CCI) and 2-dimensional monochromatic OSL-images (Hashimoto et al., 1995, 2002a). In the spectral analysis of IRSL from feldspar constituents, intense red luminescence emission has been shown in wavelengths longer than 600nm, as well as 550nm and 580nm broad peaks.

Since the IRSL from feldspars is very effectively bleached with sunlight at deposition (Aitken, 1998), the IRSL-dating of feldspars is a useful addition to the dating of Quaternary-sediment layers. In the present paper, the imaging technique of red-IRSL (R-IRSL) phenomena was developed for feldspar samples and a granite slice. Subsequently, further quantitative measurements of R-IRSL were carried out after reduction of background events as low as possible by means of the careful selection of filter-combination. R-IRSL enhancement from two kinds of feldspars has been examined by applying thermal annealing treatments in oxidative or reductive environments

Experimental

1. Preparation of samples

Slice and grain samples of granite rock and two kinds of feldspars, were prepared from: 1) An HW-2 granite, mylonite-like sub-facies (granodiorite), originated from Hanawa pluton zone adjacent to Tanakura Shear Zone, Fukushima, Japan, 2) a microcline (potassium feldspar) was of pegmatite origin, Nellore, Andhra Pradesh, India, and 3) an albite feldspar was obtained from Itoigawa, Niigata, Japan. The HW-2 specimen has almost the same origin as sample HW-5 in a previous paper (Hashimoto et al., 2002a).

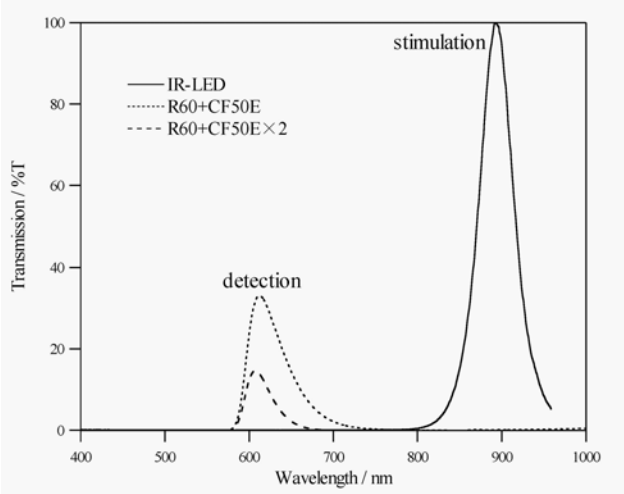

Figure 1.
Spectral response of infrared from light emitting diode (LED) for stimulation and filter assemblies for red-IRSL detection.

After cutting roughly into rectangular planes (approximately 30x20x0.5 mm), each surface was polished with an alumina emulsion solution. Small feldspar disk slices (less than ϕ=5mm) were subjected to IRSL-spectrometry. Every sliced rock sample was followed by X-ray irradiation. The feldspar pieces were also crushed to prepare grain samples (ϕ=150-250μm) for the measurements of R-IRSL decay curves associated with thermal annealing treatments. Thermal annealing treatment was performed in oxidative and reductive conditions for 3 hr at about 900°C. To attain reductive conditions, the inner atmosphere of the quartz capsule containing the grain samples was replaced with nitrogen gas and annealing was achieved in the presence of graphite powder. In the case of oxidative conditions, the sample grains were annealed in atmospheric air.

2. Observation of IRSL color images and spectrometry

All luminescence color images were observed after irradiation from an X-ray generator (Philips, PW 1830), of which the exposure rate was standardized with a ^{137}Cs standard γ-ray source (Pony Co. Ltd., PS-3000 SB Type). Following X-ray irradiation with an absorbed dose of 200-800 Gy (for 5-20 min exposure time), slice samples were "cooled" to remove completely afterglow emission, by letting the samples stand for 1 day or more in a dark box. The IRSL-color imaging (IRSLCI) observation of the slice samples was carried out by means of a photographic assembly, interposing a cold filter (Kenko CF) between camera and sample, as described in Hashimoto et al. (2002a).

An on-line spectrometric system for extremely weak photon-emission was used for the spectrometry of IRSL from pieces of feldspar slice in the similar way to the granite ones (Hashimoto et al., 1997; 2002a). Every scanning interval was 22 msec and 512 channel data (in wavelength) were summed up to 45 cycles to form one spectrum per second. Thus, 100 spectra during the period of 100 sec stimulated with IR-light, could be acquired to the microcomputer memory. All of the spectrum data were plotted in a spectrum for every slice sample.

3. Red IRSL measurement

Sixteen LEDs (IR-LED, Hamamatsu Photonics, L2690-02), with 890 nm emission peak with 50 nm FWHM value, were installed to an LED holder having a hole of 10 mm in diameter. This IR-LED holder was fixed to an automatic system for the TL and OSL measurement equipped with a small X-ray irradiator (Hashimoto et al., 2002b). The applied IR power was measured to be 27 mW/cm^2 at the surface of the grain samples in a silver pan (ϕ=8mm), in which about 5 mg of feldspar grains was placed for every measurement. The optical properties in transmission of the filter combination and stimulation light from the IR-LED are shown in Fig. 1. To keep background events as low as possible, the transmittance of stimulated IR-LED light should be excluded completely from the low-wavelength tail of the 890nm-emission peak. A photomultiplier tube (Hamamatsu Photonics, R-649S) installed in a cooling box at -20°C is sensitive to long wavelengths owing to a multialkali surface. Since this photomultiplier tube is sensitive even to infrared light, two cold filters (Asahi-techno Glass, CF-50E) were used. In these conditions, the mean background counting rate under the illumination of 16 IR-LEDs amounted to 580 counts per 0.1sec data acquisition period.

All R-IRSL measurements were carried out at 125°C after preheating for 3min at 220°C after the artificial irradiation. The dose-response curves were obtained using a single aliquot regenerative (SAR) method (Aitken, 1998) with correction for sensitivity change using a test dose of 10.5Gy.

Results and discussion

1) IRSL color images

Infrared-stimulated luminescence color images (IRSLCI) of the X-ray-irradiated granite and microcline slices are presented in Fig. 2.

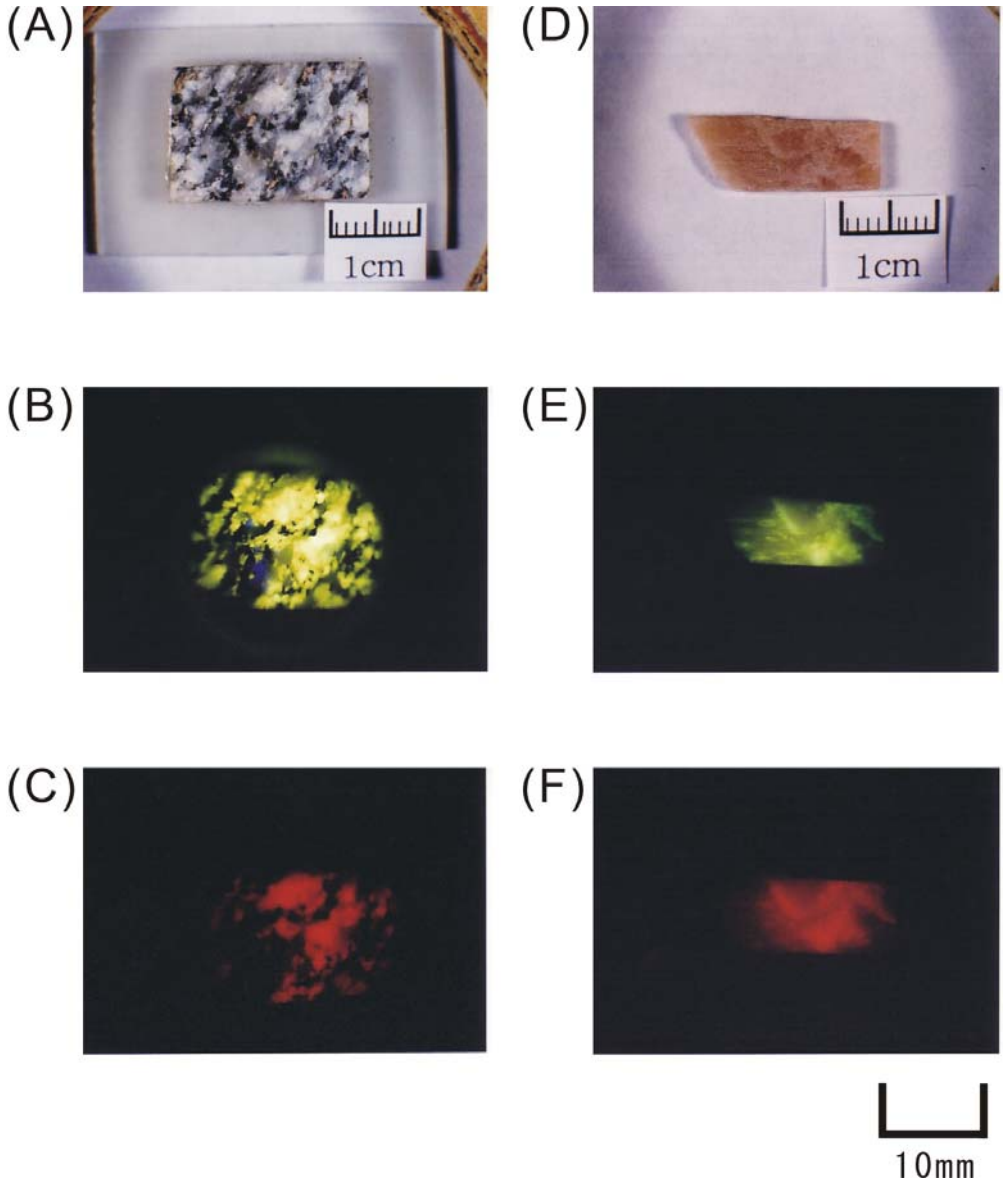

Figure 2.
Typical infrared stimulated luminescence color images (IRSL-CIs) from granite and microcline slices. Real surface images, (A) and (D), are from granite (HW-2) and microcline (India) slices, respectively. Two yellowish IRSL-CIs, (B) and (E), were photographed in visible light regions by interpolating a filter (CF 50E) between camera and slice sample, under illumination by infrared light from LED. Two reddish IRSL-Cis, (C) and (F), were photographed by interpolating an additional filter (R-60). Both slices were irradiated with X-rays to a dose of 200Gy and left for more than one day before photography.

In the granite IRSLCI (B), feldspar (microcline or plagioclase) portions in the real images tend to cause strong yellowish luminescence with IR-illumination, in good agreement with the afterglow and thermoluminescence color images (Hashimoto et al., 1995). There appear faint violet-colored parts, probably due to quartz portions. Although the IRSLCI of granite has been ordinarily observed as either yellow or faint violet (blue), the subsequent experiments proved, with fair certainly, red and faint violet IRSL emission from all feldspar samples. In fact, R-IRSLCI (C) was obtained on the same granite slice by interposing a red filter (Toshiba, R-60) between the sample and camera. Similar IRSLCIs were confirmed on the microcline slice (D-F) and

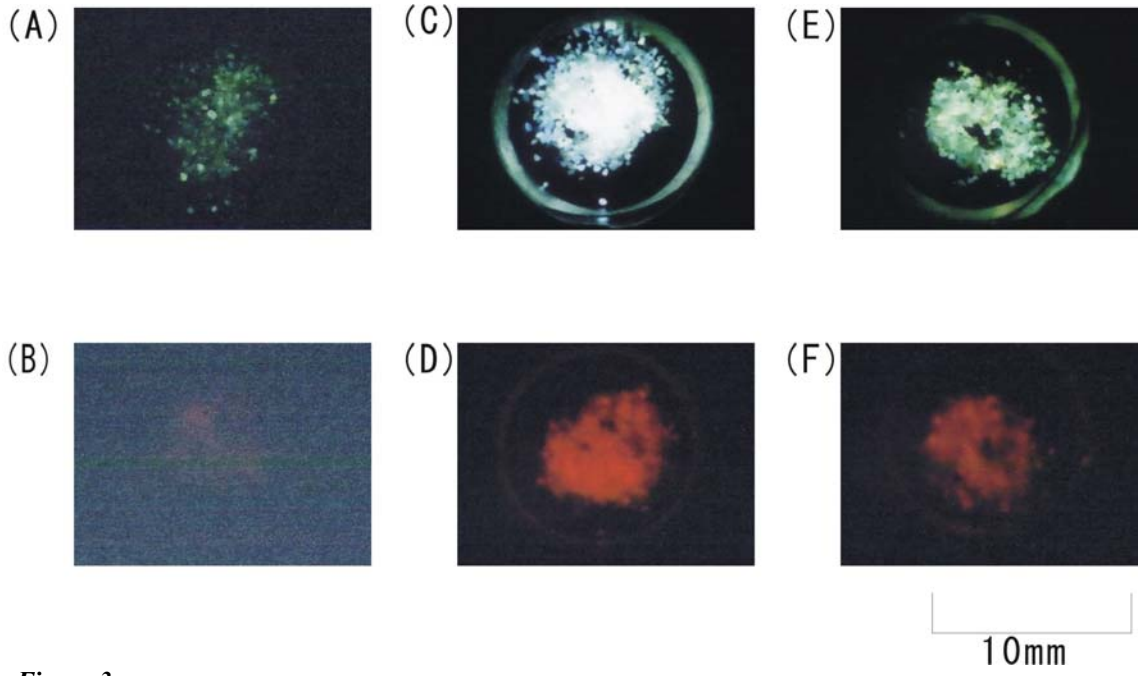

Figure 3.
Dependence of the IRSLCI from albite grain samples on annealing treatments.
Three upper images, (A), (C), (E), and three bottom images, (B), (D), (F), are taken without and with interposing the R-60 filter, respectively. Images (A) and (B) are obtained from as-received albite grains. (C) and (D) images (E) and (F) following thermal annealing treatments in oxidative and reductive condition, respectively, for 3h at 900^{o}C. All samples received of 800Gy of X-rays.

albite grain samples as seen in Figs. 3(A) and (B). Both yellowish and red-IRSL color images show heterogeneous distributions analogous to afterglow and thermoluminescence with feldspar slices (Hashimoto et al., 2001). It should be emphasized here that even natural or as-received samples of both microcline and albite feldspar are emitting R-IRSL

In Hashimoto et al., (1995), albite, potassium and plagioclase feldspar constituents in granite were recognized to be highly sensitive to radiation-induced luminescence, involving radio-luminescence (RL), TL, afterglow, photo-induced phosphorescence as 2-D color images. On the other hand, quartz showed a relatively weak sensitivity to luminescence phenomena even in the color center images and radioluminscence (Hashimoto et al., 2003). The present results support the especially intense luminescence sensitivity of the feldspar portions.

Additionally, it is suggested that light-sensitive trapped electrons (and hole centers) in minerals should greatly depend on the conditions of thermal annealing treatments. The IRSLCIs from albite grain samples, which were annealed with oxidative or reductive conditions, are shown in Fig. 3(C)-(F). It is verified that all of the IRSL-images are enhanced after the annealing treatments, particularly in the R-IRSLCIs. From the annealed sample in oxidative conditions, both visible light in Fig. 3(C) and R-IRSLCIs (D) are enhanced more than the corresponding IRSLCIs in the case of reductive conditions, as indicated in Fig. 3(E) and (F).

2) IRSL-spectra of feldspars

Further quantitative spectral information could be obtained by means of on-line spectrometry. Three spectral results are shown in Fig. 4. Since the luminescence phenomena appear immediately after the IR-LED exposure, the spectra should change from strongest spectrum, which appears in the uppermost spectrum, to weaker ones in the vicinity of final IR-illumination time of 100sec. In the figures the spectra are superimposed upon each other. In agreement with Hashimoto et al. (2002a), the spectra from feldspars consist of a prominent yellowish emission having a peak at 550 nm and orange color having a peak at 580nm. In addition to these peaks; a violet emission emerges at wavelengths shorter than 450nm and another (red) on the long wavelength side beyond 600 nm. The latter emission must correspond to the R-IRSL images as mentioned above in photographs and the spectrum of this is assumed to give a peak at 750nm as expected from afterglow

spectral results (Hashimoto et. al., 2001). Two models of a broad red luminescence around 750nm in feldspars have been suggested: a reaction of the reduced state (Fe(II)) into the oxidation state (Fe(III)) of iron-impurity, alternatively, secondary emission of the Fe(III) excited state, induced by blue photons (Kirsh and Townsend, 1988).

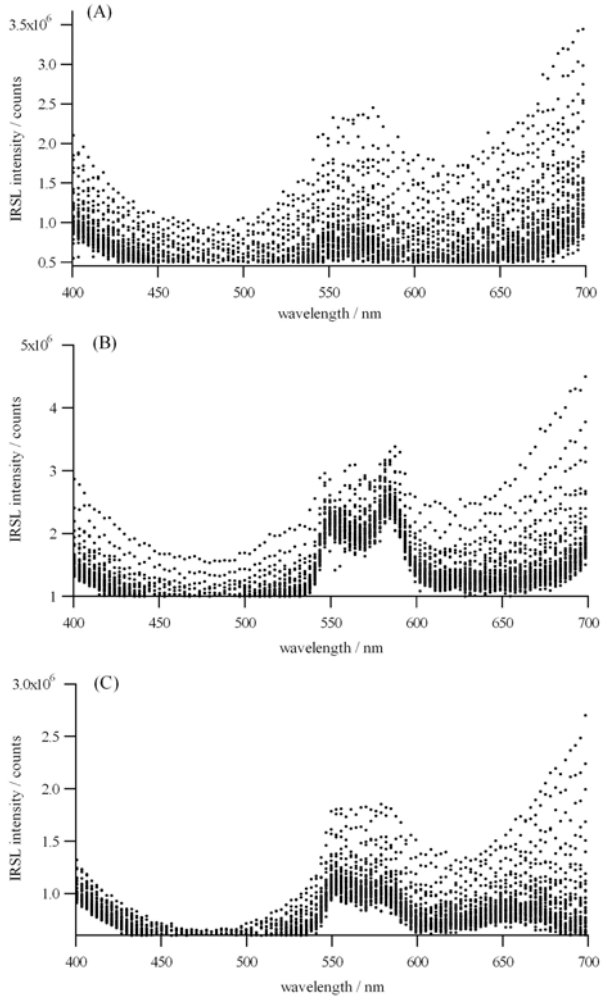

Figure 4.
IRSL-spectra from feldspars by on-line spectrometry with an image intensifier. Every spectrum consists of 100 spectra displaying the decaying behavior of IRSL after start of IR-LED illumination. Feldspar samples are (A) microcline, (B) albite (as-received,) and (C) albite annealed in oxidative conditions. All specimens were exposed to X-rays to doses of 400-800Gy. Each data point consists of photon-counts per 0.1sec interval.

With this in mind, IRSL spectrometry was performed for the thermally annealed albite sample. The spectra are illustrated in Fig.4(C), in which the sample was annealed under oxidative conditions. An enhancement in the red emission regions, by comparison with the yellow emission regions, is clear (c.f. Fig. 4(B)). This result suggests an increase of iron-oxidation state, associated with the oxidative annealing conditions.

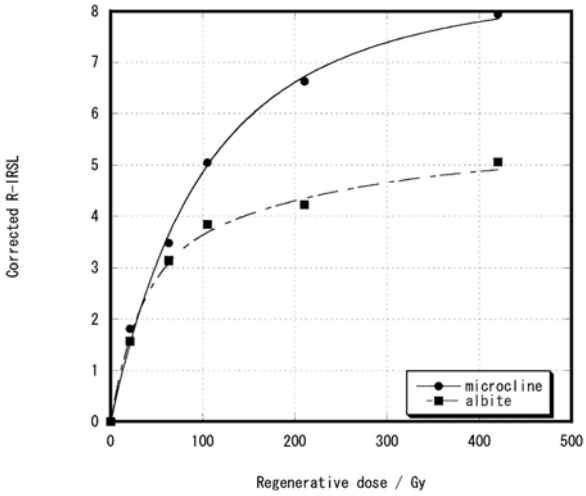

Figure 5.
Growth curves of R-IRSL against additive doses for microcline and albite grains. These two samples were thermally annealed in oxidative conditions. IRSL intensities were integrated for 1 sec of decay curves and corrected by those of the test dose (10.5Gy), of which measurements were carried out between additive dose procedures.

3) Dose response of R-IRSL

To make R-IRSL dose-response curves the R-IRSL values integrated during 1 sec exposure period are plotted in figure 5 against regenerative doses after correction of sensitivity change from IRSL-intensities with the test dose. The final response curves for both microcline and albite samples, which are thermally annealed, are shown. Microcline gives slow saturation trends beyond about 100Gy, whereas albite tends to be saturated rapidly, even at doses less than 100Gy.

This dose-response information of annealed feldspars will be useful for the application of R-IRSL to dating of archaeological porcelain pieces and burnt stones which contain a lot of feldspar constituents, and which might have experienced either oxidative or reductive conditions in their manufacture.

To obtain the optimal measurement of R-IRSL, the detection window widths must be extended into longer wavelength regions by applying the appropriate filter combinations, as well as the reduction of background due to IR-LED as low as possible.

Acknowledgements

The present work was supported greatly by Grant-in Aids for Fundamental Science Research from the Ministry of Education and Culture, Japan (No. 14340231).

References

Aitken, M. J.. (1998). An Introduction to Optical Dating: The Dating of Quaternary Sediments by the Use of Photo-Stimulated Luminescence. Oxford University Press, Oxford.

Clarke, M. L. and Rendell, H. M. (1997). Stability of the IRSL spectra of alkali feldspars, *Physica status solidi (b)*, **199**, 597-604.

Hashimoto, T., Notoya, S., Ojima, T., Hoteida, M., (1995). Optically stimulated luminescence (OSL) and some other luminescence images. *Nucl. Tracks Radiat. Meas.*, **24**, 227-237.

Hashimoto, T., Sugai, N., Sakaue, H., Yasuda, K., Shirai, N., (1997). Thermoluminescence (TL) spectra from quartz grains using on-line TL-spectrometric system. *Geochem. J.*, **31**, 189-201.

Hashimoto, T., Yamazaki, K., Morimoto, T., Sakaue, H., (2001) Radiation-induced luminescence color images from some feldspars *Anal. Sci.*, **17**, 825-831.

Hashimoto, T., Usuda, H., Yawata, T., (2002a) Color images of infrared stimulated luminescence (IRSL) from granite slices exposed to radiations. *Ancient TL*, **20**, 19-23.

Hashimoto, T., Nakagawa, T., Hong, D. G., Takano, M., (2002b) An automatic system for both red/blue thermoluminescence and optically stimulated luminescence measurement. *J. Nucl. Sci. Technol.*, **39,** 108-109.

Hashimoto, T, Yamaguchi, T, and Yanagawa, Y. (2003) Comparison of infrared spectrometric characteristics of Al-OH impurities and thermoluminescence patterns in natural quartz slices at temperature below 0^{o}C Radiat. Meas., in press.

Hütt, G., Jaek, I., Tchonka, J., (1988). Optical dating: K-feldspars optical response stimulation spectra. *Quatern. Sci. Rev.*, **7**, 381-385.

Kirsh, Y. and Townsend, P. D., (1987) Local transitions and charge transport in the thermoluminescence of calcite. *Nucl. Tracks Radiat. Meas.*, **13**, 115-119.

Krbetschek, M. R., Goeze, J., Dietrich A., Trautmann T., (1997). Spectral information from minerals relevant for luminescence dating. *Radiat. Meas.*, **27**, 695-748.

Reviewer

J. Prescott

Influence of radiation used by the security control at airports on the TL signal of quartz

M. Haustein[1], M.R. Krbetschek[2], E. Pernicka[1]

[1] TU Bergakademie Freiberg, Institute of Archaeometry, Gustav-Zeuner-Str. 5, D-09596 Freiberg, Germany
[2]Saxon Academy of Sciences, Quaternary Geochronology Section at TU Freiberg, Bernhard-von-Cotta-Str. 4, D-09596 Freiberg, Germany

(Received 25 September 2002 ; in final form 25 December 2002)

Abstract *In some cases samples for luminescence age determination have to be transported by plane. At all airports these samples have to pass a security control. For this purpose the baggage is X-rayed. In the past it was assumed that a low X-ray dose, as used in the case of security controls, does not influence the luminescence signal. However, in this paper an example is given for quartz from archaeometallurgical slag that is strongly influenced by the radiation used in security checks. Tests were carried out on sample material that passed a simulated security control at Dresden Airport. From these measurements we obtain evidence that the radiation influences the TL signal. The consequence may be a complete change of the luminescence signal, which would lead to a dating error.*

Introduction

Since the 11th of September 2001 the intensity of security controls has strongly increased. Especially the transport by plane includes security checks using X-rays. The doses applied are in a range of µGy in case of the low dose X-ray systems (Heimann Systems GmbH) or much higher in case of high dose X-ray scanners (InVision Technologies INC). The X-radiation might be not much different in energy from γ-radiation, but it is important that the low dose given to the sample in nano- or milliseconds, leads to very high dose rate. Thus, the effect on the TL properties of a sample can be completely different from β- or γ-radiation used in the case of luminescence dating.

A first suspicion of X-ray influence arose with quartz isolated from slag samples from Cyprus, which were transported by plane to Germany. The TL signals measured appeared unusual. It was impossible to determine an exact palaeodose from the glow curves. By excluding all other possibilities an influence of X-rays used by the security check at Larnaca airport was suggested to explain this phenomenon. In order to validate this possibility a security check was deliberately passed at Dresden airport with a slag sample with a well known TL behaviour.

The slag samples from Cyprus

As part of a research project for dating archaeometallurgical slags by TL (Haustein 2002 and Haustein and Krbetschek, 2002) six slag samples from ancient slag heaps on Cyprus were taken. To protect the samples from light, the slags were packed into metal containers. For transport by plane the samples were added to the baggage and hence, they passed the security control at Larnaca Airport.

In the laboratory quartz grains were separated from the slag body by a procedure described by Haustein and Krbetschek (2002). The preparation includes crushing and sieving of the sample, followed by density separation and etching with aqua regia and hydrofluoric acid. With this procedure quartz grains with sizes ranging from 90 to 125 µm were obtained. TL measurements were carried out on the separated quartz grains using a Risø TL 8 unit. For determination of the palaeodose the red TL (RTL) emission at about 620 nm combined with a single aliquot regeneration technique (SAR protocol) was employed. The conventional bialkali PMT was replaced by a trialkali PMT SbKNaCs type RFT M12FC51 (equivalent to EMI 9558B). For cutting out the RTL emission an optical interference filter type LOT-ORIEL D630 with 85% transmission in the range 605-650 nm was chosen.

For the regeneration of the natural signal it was necessary to irradiate the sample with a β-dose of about 290 Gy. An exact determination of the palaeodose was not possible because of the small plateau range (Figure 1). Additionally the natural glow curves were untypical for quartz. Especially the peak at 210 °C (heating rate 3 K/s) was completely missing, while this peak was present in regenerated signals. For general information about typical TL emissions of quartz see e.g. Krbetschek et al. (1997).

Most of the slag samples from Cyprus are from the roman period or later. Therefore a palaeodose of 290 Gy is impossible since the dose-rate determined was about 1 Gy/ka. The glow curves of the six samples from Cyprus are similar to one another. The natural and the regenerated signal of sample Z2 (Figure 1) gives an example for all of the other quartz samples.

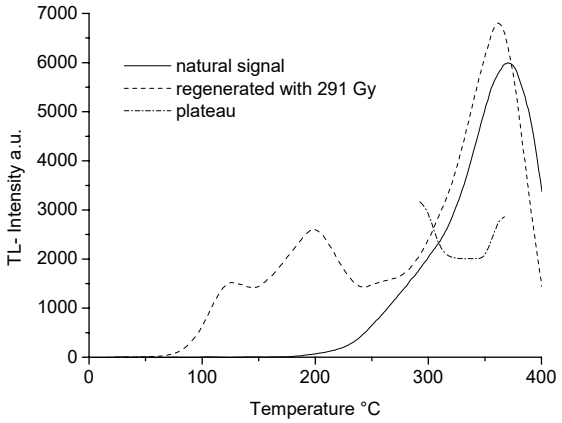

Figure 1.
Natural and regenerated glow curve of quartz from sample Z2 from Cyprus (RTL-signal, heating rate 3K/s). For regeneration a β-dose of about 290 Gy was needed. The dose-rate was determined about 1 Gy/ka. Thus, it is impossible that the sample has accumulated such a high palaeodose. To explain the effect an influence by X-rays used at security control was suggested.

By measuring samples from other locations prepared by the same procedure as in the case of samples from Cyprus, the effect was not found. Therefore, we can be sure that the quartz-separation procedure did not change the TL sensitivity. Since the grains used for TL measurements are included in large slag aggregates during sampling and transport light exposure is unlikely. The only difference was that all other samples were not transported by plane so that we suspected that the security control at the airport was the reason for the dubious phenomenon. To test this assumption a reproduction of the effect was necessary.

Simulation of security control and palaeodose measurement

Unfortunately it was not possible to repeat the security control at Larnaca airport. There is also no exact information about the procedure used because all informations concerning security are kept secret. Alternatively we simulated a security control by using a low-dose X-ray scanner HI-SCAN 6040 from Heimann Systems at Dresden Airport. The dose of this system is about 2 µGy with an energy of about 140 keV (Heimann Systems, 2002). Although it was clear that we can not reproduce the conditions of the earlier exposure exactly, because it was suspected that different instruments were used at Dresden and Larnaca Airports.

A slag sample from the old smelting site "Versunkene Kirche" in Austria (see Presslinger 1998), with a well known natural TL signal (Haustein 2002) was divided into two parts called Oe11 and Oe11 SC (SC=**S**ecurity **C**ontrol). The sample Oe11 SC was packed into a metal container and added to a baggage as typical for air travel. This baggage was subjected to a security check by the German Federal Border Guard (BGS) at Dresden Airport. The second part of the slag (Oe11) was not exposed to artificial radiation.

In the next step the quartz was separated from the two samples. The TL measurements were carried out using a Risø TL 12 unit with a bialkali PMT type EMI 9635. An optical interference filter type SCHOTT OG 530 was employed. The glow curves of natural RTL obtained from sample Oe11 and Oe11 SC (mean of ten aliquots with 1-sigma standard deviation) are shown in Figure 2.

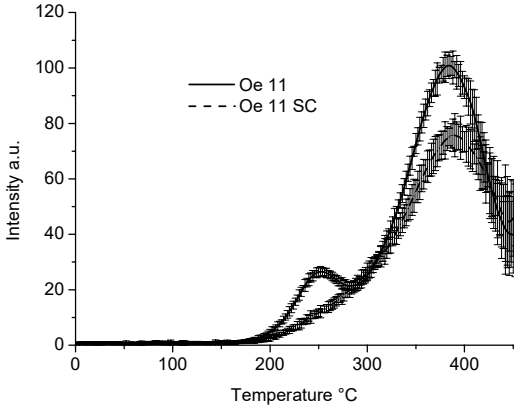

Figure 2.
Glow curves of quartz from sample Oe11 and Oe11 SC (RTL signal, heating rate 10K/s). Mean of ten measurements with 1-sigma standard deviation. Security control was simulated on sample Oe11 SC by the Federal Border Service at Dresden Airport. The signal intensities differ significantly from one another. As found in the samplesfrom Cyprus, in the X-rayed slag the peak at about 250°C is completely absent.

After measuring the natural RTL the heated aliquots were irradiated with β-doses (Sr-90 source). The glow curves of Oe11 and Oe11 SC obtained after a radiation dose of 17 Gy are given in Figure 3. They

were performed by mean of 10 measurements. In addition to the regeneration technique (SAR) an additive irradiation was carried out. The additive glow curves with the determined plateau areas of Oe11 and Oe11 SC are shown in Figures 4 and 5.

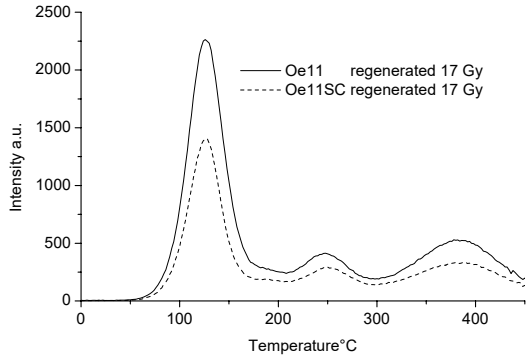

Figure 3.
Regenerated glow curves (17 Gy β-dose) of quartz from sample Oe11 and Oe11 SC (RTL signal, heating rate 10K/s). Mean of ten measurements. For clarity of the figure the signals are shown without error bars. The regeneration of X-ray influenced sample leads to a lower TL intensity as in the case of not influenced sample.

Results and **Discussion**

The natural glow curves of the sample exposed to X-rays and the unexposed sample (Figure 2) differ significantly. The glow curve of Oe11 is typical for heated quartz, with peak maxima at about 250 and 380°C (heating rate 10K/s). In contrast, the glow curve of Oe11 SC rises to 390°C, without a maximum at 250°C. Additionally, the intensity is lower than for the unexposed sample. For typical TL signals of quartz see Scholefield and Prescott (1999) or Fattahi and Stokes (2000).

In Figure 3 the regenerated glow curves of the two samples are shown. It is obviously that the β-dose applied to Oe11 SC results in a lower signal than in Oe11, i.e. to obtain the same signal intensity a much higher dose is necessary. The glow curves obtained from the two samples by an additive irradiation are also very different. For Oe11, the natural signal and the signals determined after an additive irradiation of 4.25, 8.5 and 17 Gy are shown in Figure 4. A good plateau was found in the temperature range from 300 to 390°C. Again much lower signal intensities were found in glow curves of Oe11 SC (Figure 5). Thus, the results of the regeneration experiment (Figure 3) could be confirmed.

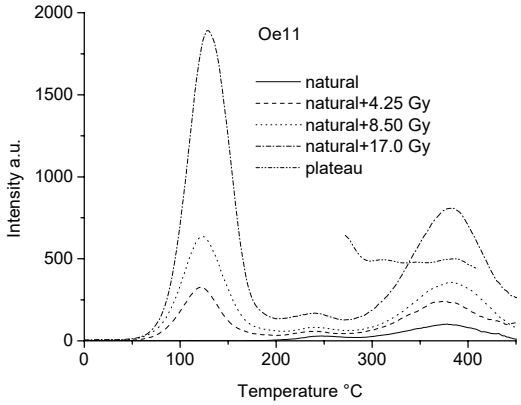

Figure 4.
Additive dose growth of TL signal of quartz from sample Oe11 (RTL signal, heatingrate 10K/s). The plateau was determined in the range from 300 to 390°C.

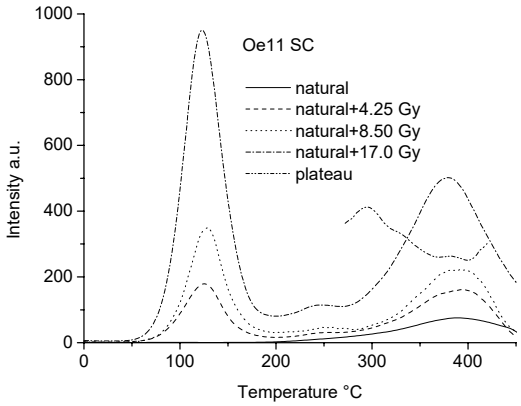

Figure 5.
Additive dose growth of TL signal of quartz from sample Oe11 SC (RTL signal, heating rate 10K/s). A plateau was found only in the small temperature range from 360 to 390°C. The signal intensity is significant lower than in the case of the not X-ray influenced sample Oe11 (Figure 4).

It is important to note that the regeneration of the X-rayed sample Oe11 SC with a β-dose of 17 Gy leads to a lower signal intensity compared with sample Oe11 which was not exposed to X-rays (Figure 3). This means that for regeneration of the natural TL signal of Oe11 SC a higher dose is necessary. Similar to the Cyprus samples the determined palaeodose of the X-rayed sample becomes too high. Additionally the natural signal after X-raying at Dresden airport is very similar to the signal of Cyprus samples (Figure 1 and 2). The 250 °C peak, typical for heated quartz in the RTL, is completely absent.

The plateau of Oe11 SC is in a very small temperature range from 360 to 390°C (Figure 5), so that the palaeodose could not be exactly determined. Nevertheless, by applying the SAR-technique in the range from 300 to 390°C a palaeodose of 6.8±0.8 Gy (mean with 1-sigma standard derivation) could be calculated, while for Oe11 5.4±0.3 Gy was observed. By use of the additive technique 6.1 Gy for Oe11 SC and 5.0 Gy for Oe11 were found. These results show that the exposure of samples to X-rays in security controls results in higher palaeodoses. Qualitatively these observations are identical to those observed in our samples from Cyprus.

Summary

Anomalous TL signals were found on quartz separated from slags that were transported from Cyprus by plane. The palaeodoses determined were unexpected high. To explain this phenomenon an influence on the TL properties of the slag material by X-rays used for security control was suggested. To validate this assumption the effect had to be reproduced. Therefore a slag sample with a well known TL signal was X-rayed at Dresden airport. As in the case of samples from Cyprus after X-raying the palaeodoses determined were to high. Additionally the TL signals look very similar to the glow curves of Cyprus samples. The peak at about 250 °C is absent. Thus, there is evidence that X-ray as used for security checks may lead to an influence on the red TL signal of quartz. There is no exact explanation of this phenomenon at the moment. A likely scenario might be a competition effect leading to de-sensitization of the luminescence from the material.

It must be pointed out that the effect is found on quartz included in slag matrix. There is no information if this or a similar phenomenon can be observed for other sample types or emissions. However, the exposition of sample material by X-ray should be strongly avoided.

Acknowledgements

The authors are very thankful for the possibility to simulate a security control at Dresden Airport by the German Federal Border Guard (BGS). We thank also Heimann Security Systems (Wiesbaden, Germany) for assistance in technical questions.

References

Haustein, M. (2002) Lumineszenzdatierungen an historischen Metallhüttenschlacken. PhD Thesis, Technical University Bergakademie Freiberg.

Haustein, M. and Krbetschek, M. (2002) Red Thermoluminescence of Quartz and its Application in Dating Archaeometallurgical Slag. *Radiation Protection Dosimetry* 101, 375-378.

Heimann Systems GmbH, Headquarters, Im Herzen 4, D-65205 Wiesbaden, Germany. Informations via Internet and Telephon, http://www.heimannsystems.com.

InVision Technologies INC, US Headquarters, 7151 Gateway Boulevard, Newark, CA 94560 Informations via Internet, http://www.invision-tech.com.

Krbetschek, M. R., Götze, J., Dietrich, A. and Trautmann, T. (1997) Spectral Information from Minerals relevant for Luminescence Dating. *Radiation Measurements* **27**, 695-748.

Presslinger, H. (1998) Schlackenkundliche Untersuchungen von bronzezeitlichen Schlacken aus dem Paltental. *Res Montanarum* **19**, 17-24.

Scholefield, R. B. and Prescott, J. R. (1999) The red thermoluminescence of quartz: 3-D spectral measurements. *Radiation Measurements* **30**, 83-95.

Reviewer

S. McKeever

Inductively-Coupled Plasma Mass Spectrometry (ICP-MS) for dose rate determination: some guidelines for sample preparation and analysis

Bailey, R. M., Stokes, S. and Bray, H.
Oxford Luminescence Research Group, School of Geography and the Environment, University of Oxford, Mansfield Road, Oxford, OX1 3TB, UK.

(Received May 2002 ; in final form 6 February 2003)

Background

We have recently started using Inductively Coupled Plasma Mass Spectrometry (ICP-MS) as a part of our evaluation of environmental dose rates and report our method here for the benefit of others who may wish to use this promising technique. As with most analytical procedures, there are a combination of advantages and disadvantages to this method (Table A1). The method allows high precision determination of radionuclides from relatively small samples (>10mg), which is clearly advantageous if sample size is limited. Further, owing to the short range (c. ~2mm) of β-particles, the calculation of β-dose from small (representative) samples is likely to be more accurate than that calculated from in situ γ-spectrometry, as the γ-range (>50cm) far exceeds the β-range. Conversely, the γ-dose calculated from a small sample will only be accurate if the sample measured is representative of the burial sediment for ~50cm in all directions (both in elemental composition and moisture content). A further potential drawback is that disequilibrium in the U and Th decay chains cannot be evaluated using ICP-MS. While it is unlikely that ICP-MS will supersede all other approaches, and indeed the most sensible strategy will be to continue a multi-techniques assessment approach, it does represent a potentially powerful complement to other methods of dose rate assessment (Aitken, 1998).

Analysis via ICP-MS

Problems have previously been associated with ICP-MS measurement of U, Th and K in sediment samples. Firstly, the instrument sensitivity required to measure K has been a long standing issue in ICP-MS research and interference from the background spectrum of the $^{40}Ar^{+}$ carrier gas has frequently limited the quality of analysis of K (Potts, 1987). Secondly, problems have been described in silicate mineral sample digestion. Specifically, it is reported (Preusser and Kasper, 2001; Yokoyama et al., 1999) that the use of hydrofluoric (HF) and nitric (HNO_3) acid digestion may result in the formation of fluoride precipitates, which inhibit the full recovery of certain elements (particularly the highly insoluble ThF groups).

Recently, results were presented by Preusser and Kasper (2001) showing good correlation between U, Th and K concentrations derived from γ-spectrometry and ICP-MS measurements. Potential inaccuracies introduced by incomplete sample digestion (as described above) were avoided by using a 22M HF and 10M $HClO_4$ (perchloric acid) solution in the digestion procedure (HNO_3 being used to suppresses the formation of insoluble fluoride precipitates). The sample was subsequently evaporated in a 6M HCl and 5.5M HNO_3 solution and finally dissolved in HNO_3 prior to measurement. While a perchloric acid digestion ensures complete digestion, its potentially explosive character (e.g., on contact with organic material; Schumacher (1960)), and the limited availability of perchloric acid-safe fume hoods, in our view make it less preferable to alternative strategies.

Over the past few months we have experimented with various sample preparation methods and have converged to what we believe is a more convenient and successful method. We have chosen to use the more conventional HF and HNO_3 digestion rather than perchloric acid because of the difficult safety issues it presents (Schumacher, 1960). In order to avoid problems associated with fluoride precipitation our digestion procedure incorporates a final stage in which a small quantity of high purity concentrated Al solution (aluminium nitrate, $Al(NO_3)_3.9H_20$ in a matrix of HNO_3) is added to the sample. The mass action effect of Al, preferentially binding to the fluoride complexes, results in full dissolution of the otherwise acid insoluble fraction. For the sake of convenience we list our approach below.

Stages of preparation

Figure 1 shows the five key stages of the ICP-MS procedure. These stages are described further in the remainder of this paper.

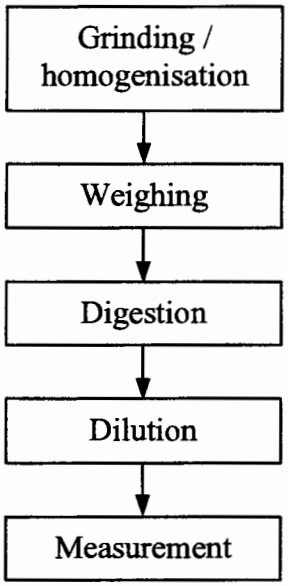

Figure 1.
Stages of the ICP-MS procedure

Grinding and weighing

Approximately 20g of raw (dry) sediment is ground in a ball mill for a 3 minutes (we use an MM200 ball mill supplied by Christison Scientific, operated at 25Hz) to reduce the sediment to a fine (<10μm) homogenised powder. Approximately 50mg of the powder is then sampled for digestion (to a precision of 0.001 mg).

Digestion

The digestion procedure is shown schematically in Figure 2 and described in detail below.

The powdered sample is placed into sealable, Teflon containers ('Teflon bombs' vol ~ 6 ml). 1.5 ml of concentrated Aristar HF (60-75%) is added to each, and the bombs are sealed and heated to 130◇C using thermostatically-controlled laboratory hot-blocks. The samples remain held at this temperature for at least 5 hours (typically overnight). After the bombs have returned to room temperature the lids are removed and the bombs re-heated at 130°C (>100°C being required for the formation and evaporation of SiF_4). After 2-3 hours the sample solutions is dried. Following evaporation, 0.2ml of concentrated (~60%) Aristar or other higher (i.e. double distilled) purity nitric acid (HNO_3) is then added to the sample. The lid is replaced and the bomb re-heated at 130°C for >3 hours. Following subsequent cooling, the lid is removed and the sample heated at 130°C to allow a further evaporation to take place. This entire procedure is then repeated.

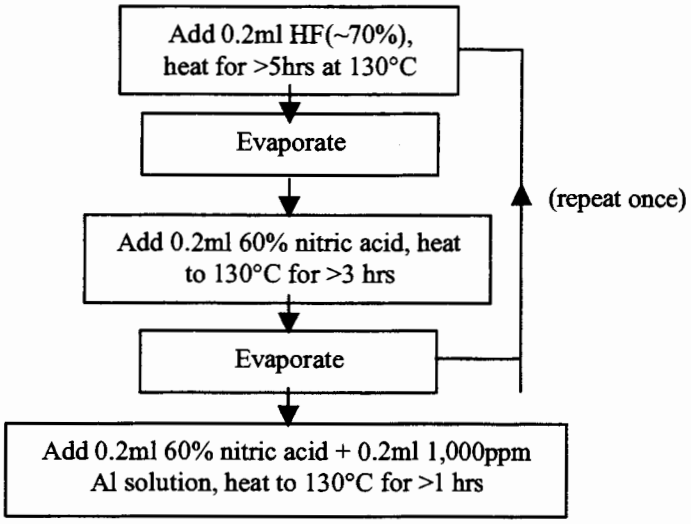

Figure 2.
Sample digestion

To the dry residual, 0.2ml of concentrated (~60%) high purity nitric acid, plus 0.6ml of high purity aluminium solution (10,000 ppm) (or equivalent) is added. The bomb is then heated (whilst sealed) at 130°C for ~ 1 hour. In the presence of aluminium, fluoride precipitates are broken down as the fluorine preferentially bonds to the aluminium and releases other elements (predominantly K and Th) back to solution. Following heating, the sample solution should be clear. If any residue remains, further heating and/or additional aluminium solution may be necessary to ensure full dissolution, although this has not, in our experience, been necessary.

Using 1% nitric acid (high purity acid diluted with high purity [18μΩ, Millipore] water), the solution can then be washed out of the Teflon bomb in to a sample tube. It is essential that a full procedural blank (full preparation, but with no powdered sample present) is measured with each batch of samples, in order to check for contamination (from, for example, impure acid). It is also good practice to measure both an internal standard (as a supplement to machine stability checks) and an external standard containing known concentrations of each measured isotope.

[1] Stoichiometically 1g SiO_2 requires 2g HF ie ~2ml 14M HF, but an excess is required to ensure complete attack of sample. 0.5-1ml 28M HF should provide a large excess.

Sample dilution and spiking

The sample is then diluted according to the requirements of the ICP mass-spectrometer being used and a 'spike' is added to the solution (in Oxford we have been using Indium) prior to measurement in order to check for unexpected matrix effects and for instrument instability.

ICP-MS Measurement

The instrument used for ICP-MS analysis was an Elan 6100 DRC Quadropole ICP-MS, which has minimum detection limits for U, Th & K of ~1 ppt (10^{-12}). The concentrations reported here were measured at ppb (10^{-9}) levels.

Testing the method

In order to test our methods, we prepared and measured a geological standard, JB1 (Japanese Basalt) using the procedures outlined above. The published values for U, Th and K concentrations of sample JB-1 are given in Table 1; our measured concentrations (the mean and standard deviation of five independent measurements) are shown for comparison. These values are shown graphically in Figure 3. As can be seen, the values obtained for JB-1 using our method agree well with the quoted values.

	U (ppm)		Th (ppm)		K (%)	
Imai *et al.* (1995)	1.67 0.28	±	9.30 0.71	±	-	
Makishima and Nakamura (1997)	1.75 0.04	±	9.66 0.23	±		
Terashima *et al.* (1996)	-		-		1.19 0.01	±
ICP-MS estimate	1.70 0.04	±	9.72 0.14	±	1.20 0.02	±

Table 1:
ICP-MS results of measurements of standard JB1. Consensus values for sample JB1 were taken from (A) Imai et al. (1995), (B) Makishima and Nakamura (1997) and (C) Terashima et al. (1996)

Conclusion

Using the method described above it is possible to obtain accurate and highly precise estimates of U, Th and K via ICP-MS. While our approach requires the use of HF, it avoids the potentially even more dangerous perchloric acid treatment most recently described by Preusser and Kasper (2001). Dose rate analysis remains a key part of luminescence dating. We believe that an ICP-MS approach offers us some advantages over and above the use of nuclear spectrometric methods such as INAA which is presently used widely.

However, as emphasized earlier, it is also helpful if dose rate estimates are based on a multi-technique strategy which allows some corroboration of results, some checks on disequilibrium, and some scope for direct measurement of α-, β- and γ-dose rates. In the absence of alternatives, and as long as samples are analysed from a homogeneous sediment context which is assumed to be in secular equilibrium with respect to U, ICP-MS provides an extremely efficient method of obtaining estimates of environmental dose rate estimates.[2]

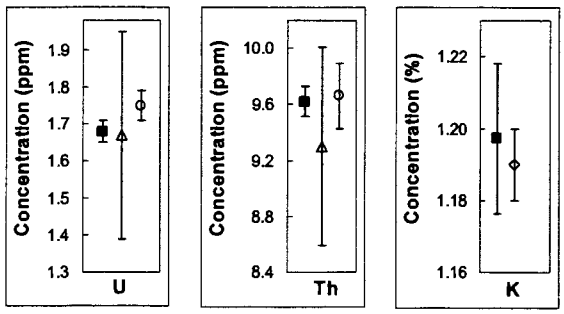

Figure 3.
The concentrations of U, Th and K measured in this study are shown as black squares. Open triangles indicate the values of Imai et al. (1995), open circles are from Makishima and Nakamura (1997); open diamond (K only) is from Terashima et al. (1996).

2

The School of Geography and the Environment offers a commercial ICP-MS service which provides analysis of U, Th & K. Costs and other details for this service are as follows:

School of Geography and the Environment
University of Oxford

ICP-MS analysis – Standard Sample analysis (assuming sampled provided ground and homogenised)

- Minimum No. of samples = 10
- Expected turn around time 4 weeks
- Analyses for U, Th & K (including duplicate runs on blanks and geological standards)
- £13 per sample

Notes:
1. Additional cost of £5 per sample if grinding is required.
2 Running smaller batches of samples or more rapid turn around periods requires negotiation

Acknowledgements

We thank Dr John Arden (Department of Earth Sciences, University of Oxford) for technical assistance with ICP-MS measurements and advice on silicate preparation. We are also grateful to Dr Andrew Murray for his helpful comments during the reviewing stage.

References

Imai, N., Terashima, S., Itoh, S. and Ando, A. (1995) 1994 Compilation of analytical data for minor and trace elements in seventeen GSJ geochemical reference samples, "Igneous Rock Series".*Geostandards Newsletter*, Vol.**19**, No.2, 135-213.

Makishima, A. and Nakamura, E. (1997) Suppresion of matrix effects in ICP-MS by high power operation of ICP: Application to precise determination of Rb, Sr, Y, Cs, Ba, REE, Pb, Th and U at ng g^{-1} levels in milligram silicate samples. *Geostandards Newsletter*, Vol.**21**, No.2, 307-319.

Potts, P. J. (1987) A handbook of silicate rock analysis. Blackie and Son Ltd (Glasgow and London).

Preusser, F. and Kasper, H.U. (2001) Comparison of dose rate determination using high-resolution gamma spectroscopy and inductively coupled plasma-mass spectrometry. *Ancient TL*, **19**, No.1.

Terashima, S., Taniguchi, M., Mikoshiba, M. and Imai, N. (1996) Preparation of two new GSJ geochemical reference materials: Basalt JB1b and Coal Fly Ash JCFA-1. *Geochemical Newsletter*, Vol.22, No.**1**, 113-117.

Yokoyama, T. (1999) Evaluation of coprecipitation of incompatible trace elements with fluoride during silicate rock dissolution by acid digestion. Chemical Geology, **157**: 175-187.

Shumacher , J.C. (1960) *Perchlorates: Their Properties, Manufacture and Uses*, American Chemical Society, Monograph Series No.**146**, Reinhold, New York

Reviewer

A. Murray

Appendix A

Technique	Quantity measured/ Result	Effective sample size	Relative cost[a]	Precision	Vulnerable to dis-equilibrium	Potential limiting factors
			Direct			
Portable (4 Ch) γ Spectroscopy	γ rays/[U], [Th], [K], ^{D}cosmic	50-60 kg	Low	Moderate-high	Yes-measures low proteges	Temp. stability, calibration
High Resolution γ Spectroscopy (HRGS)	γ rays/[U] - most isotopes, [Th] - most isotopes, [K]	30-60g	Very high	High	Disequ. directly measured	Calibration
Low Resolution γ Spectroscopy (LRGS)	γ rays/[U], [Th], [K]	500g	Low	Low	Yes	Temp. stability, calibration
Thick source α counting (TSAC)	α particles/[U], [Th]	2-3g	Very low	High	Yes-calculations assume equilibrium	Overcounting, sample representativeness
β/γ TLD	β particles or γ rays/ D_β or D_γ	Up to 50-60kg	Low-moderate	Moderate-high	Yes	Labour (during TL read out)
Thick source β counting (TSBC)	β particles / D_β	2-3g	Low-moderate	Moderate-high	Yes	Labour (during prep.) sample representativeness
			Indirect			
Flame photometry (FP)	[K]	2-3g	Very low	High	-	Calibration, sample representativeness
Neutron activation (NAA)	[U], [Th], [K]	2-3g	High (non-recurrent)	Moderate	Yes-measures parents	sample representativeness
Inductively-coupled plasma mass spectroscopy (ICP-MS)	[U], [Th], [K]	2-3g	High (non-recurrent)	Very high	Yes-measures parents	sample representativeness

Table A1

Some important factors in the selection of some commonly used dosimetric techniques

[a]The relative cost is frequently at least in part dependent upon equipment availability, purchase/maintenance and incorporates a weighting factor for duration of measurement and degree of required operator specialisation.

3

The School of Geography and the Environment offers a commercial ICP-MS service which provides analysis of U, Th & K. Costs and other details for this service are as follows:

School of Geography and the Environment
University of Oxford

ICP-MS analysis – Standard Sample analysis (assuming sampled provided ground and homogenised)

- Minimum No. of samples = 10
- Expected turn around time 4 weeks
- Analyses for U, Th & K (including duplicate runs on blanks and geological standards)
- £13 per sample

Notes:

1. Additional cost of £5 per sample if grinding is required.
2 Running smaller batches of samples or more rapid turn around periods requires negotiation

IRSL dating of K-rich feldspars using the SAR protocol: Comparison with independent age control

Frank Preusser
Institut für Geologie, Universität Bern, Baltzerstrasse 1-3, 3012 Bern, Switzerland.
preusser@geo.unibe.ch

(Received 11 March 2003 ; in final form 30 April 2003)

Abstract : *Infrared stimulated luminescence (IRSL) ages of four samples from three independently dated sites in the forelands of the Alps of Europe and New Zealand were determined using the single-aliquot regenerative-dose (SAR) methodology applied to K-rich feldspars. It is demonstrated that all IRSL ages agree well with the known age of the samples. Previously reported age underestimation of K-feldspar samples from the Rhine-Meuse delta was explained to result from increasing trapping probability caused by preheating of the natural sample. Experiments carried out for the samples investigated here, however, reveal no such increase. Hence, monitoring the trapping probability may be an appropriate test to identify K-feldspars suitable for SAR dating.*

Introduction

During recent years, the development of the single-aliquot regenerative-dose (SAR) protocol (Murray and Wintle 2000) significantly improved the precision of optically stimulated luminescence (OSL) dating of sediments. The SAR technique allows a more precise determination of the palaeodose than previously used multiple-aliquot additive-dose (MAAD) approaches. However, while the SAR method has most successfully been applied to quartz from different environmental settings (e.g. Banerjee et al. 2001, Colls et al. 2001, Fuchs and Lang 2001, Hilgers et al. 2001), when applied to K-feldspars from sediments of the Rhine-Meuse system the results systematically underestimated the expected palaeodose. In comparison with historical data and radiocarbon ages in the range 600 – 13,000 yr K-feldspars showed a systematic underestimation of up to 35 % (Wallinga et al. 2001). Experimental evidence suggested that this underestimation was caused by an increase in electron trapping probability as a consequence of preheating the natural sample (Wallinga et al. 2000a). Consequently, SAR methodology is rarely used for determination of the palaeodose of K-feldspars in luminescence dating. However, K-feldspars have some important advantages over quartz:

1) The saturation dose in feldspar is usually much higher than in quartz offering a potential to expand the range to be dated by luminescence methods.
2) The important contribution of ^{40}K within the grains to the total dose rate minimises the effect of uncertainties in the calculation of the external dose rate such as radioactive disequilibrium, water content, and cosmic dose.
3) Quartz originating from young orogenic systems such as the Alps often has poor luminescence properties, e.g. extremely low or no OSL signals. Frequently such quartz also shows large changes in sensitivity during repeated measurements that are not always corrected by the SAR protocol (Preusser 1999a, Stokes et al. 2000). Furthermore, it is difficult to deal with feldspar inclusions present in quartz from some geological provenances (Wallinga et al. 2002).

A reliable method to determine the palaeodose in K-rich feldspar would thus importantly improve the applicability of luminescence dating. It is important to notice that the investigations of Wallinga et al. (2000a, 2001) were all carried out on samples from the Rhine-Meuse system. This area lies down-stream of young volcanic rocks in the Eifel and Siebengebirge regions of western Germany. Thus, it is possible that the phenomenon causing the underestimation of K-feldspar ages is caused by the presence of volcanic feldspars, such as sanidine, in the sediment and might be absent in other geological regions. Feldspars of volcanic origin regularly show anomalous fading of the luminescence signal with time (Wintle 1973, Visocekas and Zink 1999 and references therein). However, in storage tests over periods up to six months, Wallinga et al. (2001) found evidence for only very limited fading of their samples (0.970 ± 0.007).

This study presents results for four samples from the forelands of the Alps of Europe and New Zealand for which independent age control exists. A modified SAR protocol was applied to K-rich feldspars using infrared stimulation.

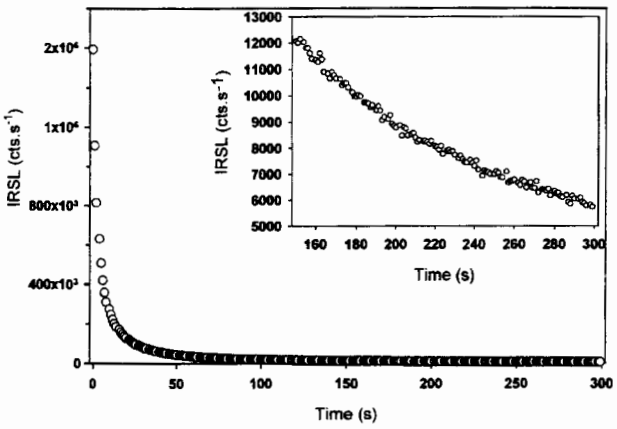

Figure 1.
IRSL decay curve for sample SHB1. The inset figure shows the latter part of the decay with an enlarged scale. Even after 150 s of IR exposure a further depletion of the IRSL signal is observed, but it is small in comparison to the initial signal.

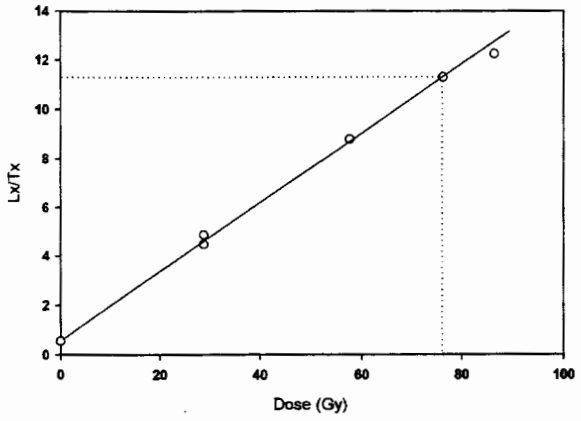

Figure 2.
Example of a dose response curve for an aliquot of sample GOS4.

Modified SAR protocol

Determination of the palaeodose was carried out using a modified SAR protocol following Murray and Wintle (2000) and Wallinga et al. (2000b). The SAR cycle included measuring the natural dose, three regenerative doses, and a zero dose. A replicate measurement of the lowest regenerative dose was carried out at the end of each SAR cycle. After each measurement a fixed test dose was given and the resultant IRSL intensity was used for normalisation. A preheat temperature of 290° C for 10 s was applied to all samples following Wallinga et al. (2001). A cut-heat temperature of 200° C was used for the test dose measurements. Stimulation by IR LEDs (maximum power 135 mW.cm^{-2} at the sample) for 300 s was applied to reset the latent infrared stimulated luminescence (IRSL) signal within the sample. The remaining IRSL signal after 300 s of IR exposure is 0.3 % of the original signal for the example given in Fig. 1. This is a typical value for most samples investigated so far. All measurements were carried out on a Risø TL/OSL 15 reader using 90 % IR diode power and carrying out the stimulation at a temperature of 125° C. A blue transmitting filter set (Schott BG 39, Schott GG 400, Corning 7-59) was used to isolate the main emission of K-rich feldspar at 410 nm (Krbetschek et al. 1997). This filter combination differs from the one used by Wallinga et al. (2000a) that transmitted IRSL in the near-blue UV, between 320 and 480 nm. A typical dose response curve is given in Fig. 2.

For all samples, three parameters are given to characterise the performance of the SAR protocol. Dose recovery indicates how accurately a known dose from a bleached (20 h by Osram Ultra Vitalux UV lamp) and irradiated (100 s beta = 11,96 Gy) but non-heated sample is recovered by the SAR protocol described above (given in Table 1 is the average of three aliquots). The recycling ratio represents how well the procedure corrects sensitivity changes that occur during repeated measuring, dosing, and preheating cycles. This performance is expressed as the ratio of the corrected luminescence intensity (L_x/T_x) of the lowest regenerative dose that is measured twice, at the beginning and at the end of the SAR cycle. The third parameter is a measure of the IRSL emitted by a bleached, non-irradiated but preheated sample (zero dose) in relation to the natural signal (L_x/T_x (zero dose) / (L_x/T_x (natural dose)). It is given as percent of the natural signal. An ideal sample will show a dose recovery of 100 %, a recycling ratio of 1.00 and 0 % recuperation.

A preheat test was carried out on a bleached (20 h by Osram Ultra Vitalux UV lamp) and dosed (11,96 Gy) sample (Fig. 3). The measured equivalent dose is almost constant with increasing preheat temperature, although, the recuperation signal increases with temperature. Fading tests for the samples investigated here have not yet been carried out, but they are available for samples from similar settings in both Switzerland (Preusser 1999a) and New Zealand (Hormes et al. 2003). None of these experiments revealed any loss of the luminescence signal over the period investigated (at least twelve months). Furthermore, Wallinga et al. (2000b, 2001) already demonstrated that fading does not explain the age short fall of their samples.

The concentration of dose rate relevant elements (K, Th, U) within the sediment was carried out by high-resolution gamma spectrometry (Preusser and Kasper 2001). For the calculation of internal dose rates potassium contents of 12.5 ± 0.5 % were used following Dütsch and Krbetschek (1997) and Huntley and Baril (1997). An alpha efficiency of 0.07 ± 0.02

was assumed. The dosimetric data is summarised in Table 2.

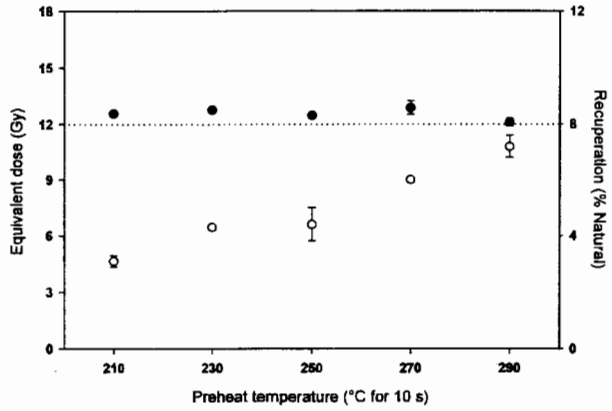

Figure 3.
Plot of equivalent dose (closed circles) and recuperation (open circles) as a function of preheat temperature (sample GOS4). The dotted line indicates the known beta dose given to the sample prior to the SAR cycle. While the equivalent dose is almost constant, recuperation slightly increases with rising preheat temperature. This does, however, apparently not effect the determination of the equivalent dose. A preheat of 290°C for 10s, giving a slightly lower but more accurate ED for sample GOS4, was applied in the dating procedure and the dose recovery test for all samples.

Dated sites and results

Four samples from three different sites were selected. In each case independent age control is available. One further sample was taken from sediment that is assumed to be older than the penultimate interglacial based on geological estimates. However, for this sample no verification of this age by other dating methods is available.

Sample GOS4 is a late Middle Würmian overbank deposit from a site near Gossau, Lake Zürich area, Switzerland. Three radiocarbon ages of 28,550 ± 310, 29,450 ± 1150 and 28,250 ± 350 ^{14}C yr have been determined for peat from just below the overbank deposit (Schlüchter et al. 1987). These radiocarbon dates represent an absolute age of *c.* 32,000 yr (Preusser et al. 2003). The U/Th age of that peat is 34,700 ± 4000 yr (Geyh and Schlüchter 1998). IRSL ages determined for the overbank deposit using the MAAD technique are 29,000 ± 3900 yr for polymineral fine-grains and 31,600 ± 3500 yr K-rich feldspars, respectively (Preusser 1999b, Preusser et al. 2003). The infrared radiofluorescence (IR-RF) age for the same sample is 32,900 ± 3400 yr (Erfurt et al. 2003).

The dose recovery experiment on sample GOS4 gave a value that was 101 ± 2 % of the known dose. Sixteen aliquots measured to determine the ED of the sample showed an average recycling ratio of 0.97 ± 0.07 and an average recuperation signal of 4.3 ± 0.7 %. The IRSL age of 28,400 ± 1900 yr determined by the SAR protocol fits well with previously calculated IRSL (MAAD) and IR-RF ages for the overbank deposit as well as with radiocarbon and U/Th dating results for the underlying peat.

Sample HURL1 originates from a sandy layer associated with sinter deposits from a site near Hurlach, Lech river valley, Bavaria, southern Germany. The Last Interglacial age of this sediment is indicated by pollen and malacological (snail) evidence as well as by an U/Th age of 120,300 ± 5800 yr (Jerz and Mangelsdorf 1989, Kovanda 1989). A previously published IRSL (MAAD) age of 134,800 ± 11,600 yr and an IR-RF age of 125,900 ± 12,200 yr (Erfurt et al. 2003) agree with both the U/Th age and biological evidence.
Dose recovery of sample HURL1 is 107 ± 2%. Eight aliquots measured for this sample show an average recycling ratio of 1.00 ± 0.15 and an average recuperation signal of 5.2 ± 0.2 %. The IRSL (SAR) age of 136,400 ± 10,500 yr agrees with independent age control.

Two samples (KMK5, KMK8) were taken from two different sandy layers within a sequence of fine-grained overbank deposits intercalating last glacial glaciofluvial out-wash gravel at a site near Kamaka, North Westland, South Island of New Zealand. A series of 14 radiocarbon ages determined for wood and plant fragments from this horizon range from 22,800 ± 200 ^{14}C yr to 21,990 ± 220 ^{14}C yr (Denton et al. 1999). This represents an absolute age of *c.* 25,000 yr when applying the calibration of Kitagawa and van der Plicht (1998).
Six and seven aliquots were measured for samples KMK5 and KMK8, respectively. Dose recovery for these two samples is 98 ± 2 % and 97 ± 0 %, respectively. The average recycling ratio is 1.10 ± 0.04 for sample KMK5 and 1.10 ± 0.08 for sample KMK8. The recuperation signal for the samples is 10.9 ± 1.3 % (KMK5) and 9.6 ± 3.1 % (KMK8). IRSL (SAR) ages of 24,300 ± 1500 yr (KMK5) and 24,400 ± 1500 yr (KMK8) agree very well with the calibrated radiocarbon age of *c.* 25,000 yr.

The estimated age of sample SHB1 from a quarry at Solenberg near Schaffhausen, northern Switzerland, is older than the penultimate interglacial (Graf, pers. com.). The sample was taken from a fluvial sediment

Sample	Origin	Dose recovery (%)	n	Recycling ratio	Recuperation. (%)	IRSL-Age (SAR) (yr)	Age control
GOS4	Gossau, CH Overbank deposit	101 ± 2	16	0.97 ± 0.07	4.3 ± 0.7	28,400 ± 1900	^{14}C: *c.* 32,000 cal. ^{14}C yr [2] U/Th: 34,700 ± 4000 yr [3] IRSL (MAAD): 29,000 ± 3900 yr [4] IRSL (MAAD): 31,600 ± 3500 yr [5] IR-RF: 32,900 ± 3400 yr [6]
HURL1	Hurlach, D Fluvial sand	107 ± 2	8	1.00 ± 0.15	5.2 ± 0.2	136,400 ± 10,500	U/Th: 120,300 ± 5800 yr [7] IRSL (MAAD): 134,800 ± 11,600 yr [6] IR-RF: 125,900 ± 12,200 [6]
KMK5 KMK8	Kamaka, NZ Overbank deposit	98 ± 2 97 ± 0	6 7	1.10 ± 0.04 1.10 ± 0.08	10.9 ± 1.3 9.6 ± 3.1	24,300 ± 1500 24,400 ± 1500	^{14}C: *c.* 25,000 cal. ^{14}C yr [1]
SHB1	Solenberg, CH Fluvial sand	106 ± 1	3	0.96 ± 0.04	2.8 ± 0.2	268,000 ± 18,000	none

Table 1.

Overview on relevant information of samples investigated in the present study. References: (1) Denton et al. (1999), (2) Schlüchter et al. (1987), (3) Geyh and Schlüchter (1987), (4) Preusser 1999b, (5) Preusser et al. (2003), (6) Erfurt et al. (2003), (7) Jerz and Mangelsdorf (1989).

Sample	Grain size (μm)	K (%)	Th (ppm)	U (ppm)	water (%)	Depth (m)	$D_{Internal}$ (Gy kyr^{-1})	$D_{External}$ (Gy kyr^{-1})	D (Gy kyr^{-1})	D_e (Gy)
GOS4	100-200	1.03 ± 0.05	8.21 ± 0.41	2.68 ± 0.13	20 ± 5	7	0.50 ± 0.16	2.01 ± 0.15	2.51 ± 0.16	71.3 ± 1.8
HURL1	100-200	1.00 ± 0.02	5.22 ± 0.24	2.67 ± 0.09	15 ± 5	1	0.50 ± 0.16	1.99 ± 0.15	2.49 ± 0.15	340.2 ± 15.7
KMK5	100-200	1.69 ± 0.05	9.14 ± 0.27	2.24 ± 0.07	25 ± 5	15	0.50 ± 0.16	2.34 ± 0.04	2.84 ± 0.16	68.9 ± 2.0
KMK8	100-200	1.49 ± 0.05	12.04 ± 0.36	2.90 ± 0.09	25 ± 5	15	0.50 ± 0.16	2.50 ± 0.06	3.00 ± 0.16	73.2 ± 2.4
SHB1	100-150	0.74 ± 0.02	3.73 ± 0.17	1.64 ± 0.06	15 ± 5	20	0.42 ± 0.08	1.64 ± 0.04	2.06 ± 0.11	550.9 ± 23.4

Table 2.

Dosimetric data, internal, external (including cosmic) and total dose rates and palaeodose for the investigated samples.

that is presumed to be deposited under cold climatic conditions. For this sample, the number of regenerative doses was increased to five allowing a better fitting of exponential dose response curves.
Dose recovery of sample SHB1 is 106 ± 1 %. Three aliquots measured for this sample show an average recycling ratio of 0.96 ± 0.04 and a recuperation signal of 2.8 ± 0.2 %. The calculated age of 268,000 ± 18,000 yr indicates a correlation with marine isotope stage (MIS) 8. From the geological point of view, this age agrees with a period of assumed cold climatic conditions.

Discussion

The dose recovery tests described here show that the modified SAR protocol works well for artificially dosed samples. Furthermore, none of the ages calculated shows any age shortfall in comparison with independent age control, in contrast to the experience of Wallinga et al. (2001) with sediments from the Rhine-Meuse system.
It may be possible that age shortfall in the different samples is masked by incomplete bleaching (Wallinga et al. 2001). However, previous experience with MAAD dating revealed that overbank deposits from different regions are usually well bleached prior to deposition (Fuller et al. 1994, Becker-Haumann et al. 2000, Fiebig and Preusser 2003, Hormes et al 2003). Similar experience is available for fluvial terrace sediments from the Alpine Foreland (Fiebig and Preusser 2001, 2003). Additionally, all samples investigated show a constant ED with stimulation time and the reproducibility of small aliquots (*c.* 50 grains) measured for the same samples is rather good (about 10 %). However, both approaches may not always allow identification of incompletely bleached samples (Aitken 1998, Wallinga 2002). For sample GOS4, complete bleaching of the IRSL signal is indicated by consistent ages determined for the silt and sand fraction (Preusser et al. 2003). Similar evidence is available for the Kamaka section by fine-grain dating of six others samples from the same site (Preusser, unpubl. data). IRSL (MAAD) and IR-RF dating confirm the IRSL (SAR) age of sample HURL1 (Erfurt et al. 2003). For the Solenberg site, five additional IRSL (SAR) ages for different samples from the same horizon agree within errors with the age of sample SHB1 (Preusser, unpubl. data). In summary, there exists different evidence that the samples were completely bleached. Thus it appears rather unlikely for the samples investigated here that age underestimation by K-feldspars is masked by the presence of a residual IRSL signal prior to deposition.

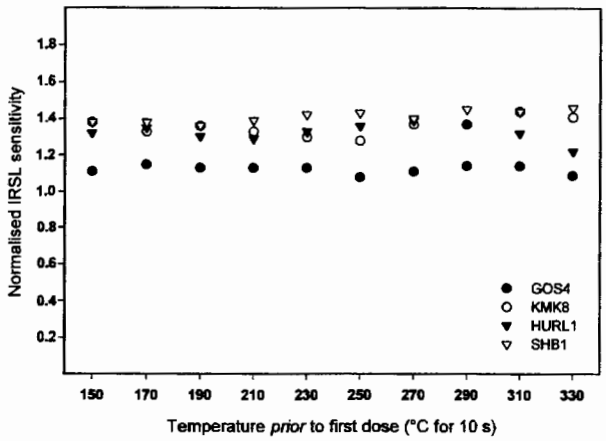

Figure 4.
IRSL response to a fixed dose as a function of the maximum temperature prior to dosing for samples from the four different sites investigated. Results are normalised to the luminescence response to the same dose in a second cycle, where all samples already experienced a heating to 290°C. In contrast to previous experience (Wallinga et al. 2000a), none of the samples showed any increase in normalised IRSL.

All the samples investigated, especially the two from Kamaka, show relatively high recuperation signals of up to 10 %. Recuperation probably results from thermal transfer of electrons (Rees-Jones and Tite 1994) and Wallinga et al. (2000b) demonstrated that the amount of recuperation is a function of preheat temperature. This is confirmed for sample GOS4 by the slight increase of recuperation with preheat temperature (Fig. 1). Anyhow, the influence on the palaeodose determination is small or even negligible as indicated for the samples investigated (Fig. 1).

Wallinga et al. (2000a) gave experimental evidence that the age underestimation of their samples from the Rhine-Meuse delta is probably caused by an increase in the trapping probability due to preheating. They undertook an experiment in which aliquots were bleached, heated to various temperatures between 25 and 275°C, given a fixed beta dose and then preheated to 290°C. The IRSL signal was then measured and this signal was normalised by giving the same beta dose and remeasuring the IRSL signal. In this experiment the normalised IRSL sensitivity increased when the temperature prior to the first dose was above 200° C, implying that the electron trapping probability had risen (Fig 5 of Wallinga et al. 2000a). Repeating this experiment for the samples investigated here reveals, however, that the IRSL sensitivity does not change with temperature prior to the first dose over the range from 150 to 330°C (Fig.

4). Thus the phenomenon that is likely to explain the previously observed age shortfall of K-feldspars from the Rhine-Meuse system, a significant change of trapping probability induced by preheating the natural sample, is not present in the samples from the forelands of the European and New Zealand Alps.

Conclusions

The case studies presented here imply that the modified SAR protocol for feldspars allows reliable dating of samples from both investigated areas. The discrepancy with previous experience (Wallinga et al. 2001) is explained by the different IRSL properties of the samples – in particular the fact that no change in the electron trapping probability is observed. It is, however, impossible to judge if this dating approach can be used for samples from other geological areas as well. There appear to be three criteria for identifying K-feldspars that are suitable for SAR dating:

1) Absence of anomalous fading. From present experience, fading is apparently linked to the presence of volcanic feldspars.
2) The ability to accurately recover the value of a given radiation dose.
3) Absence of any change in trapping probability as a function of temperature prior to dosing.

If these criteria are fulfilled one should expect to get a reliable palaeodose determination using the SAR protocol presented here. It is, however, necessary to apply the presented methodology to samples from other environments where independent age control is available.

Acknowledgements

Measurements were carried out at the luminescence laboratory of Universität zu Köln, Germany. The help and hospitality of A. Hilgers, U. Radtke and all other at the Department of Geography are highly acknowledged. R. Beckermann-Haumann provided sample HURL1. The author thanks J. Wallinga for his comments on an earlier draft of the manuscript and G. Duller for his very constructive review. This project was financially supported by the Swiss National Science Foundation (Grant-No. 21-063988.00-Schlüchter).

References

Aitken, M.J. (1998). *An introduction to optical dating*. University Press, Oxford, 267 pp.

Banerjee, D., Murray, A.S. and Foster, I.D.L. (2001). Scilly Isles, UK: optical dating of a possible tsunami deposit from the 1755 Lisbon earthquake. *Quaternary Science Reviews*, **20**: 715-718.

Becker-Haumann, R., Preusser, F., Chowdhury, K.R., Khan, S.H. and Huq, N.E. (2000). A test study of luminescence dating of fluvial sediments from Bangladesh. *Bangladesh Journal of Geology*, **19**: 24-34.

Colls, A.E., Stokes, S., Blum, M.D. and Straffin, E. (2001). Age limits on the Late Quaternary evolution of the upper Loire River. *Quaternary Science Reviews*, **20**: 743-750.

Denton, G.H., Heusser, C.J., Lowell, T.V., Moreno, P.I., Anderson, B.G., Heusser, L.E., Schlüchter, Ch. and Marchant, D.R. (1999). Interhemispheric linkage of paleoclimate during the last glaciation. *Geografiska Annaler*, **81A**: 107-153.

Dütsch, C. and Krbetschek, M.R. (1997). New methods for a better internal ^{40}K dose rate determination. *Radiation Measurements*, **27**: 377-381.

Erfurt, G., Krbetschek, M.R., Bortolot, V.J. and Preusser, F. (2003). A fully automated multi-spectral radioluminescence reader system for geochronometry and dosimetry. *Nuclear Instruments and Method in Physics Research B*. (in press)

Fiebig, M. and Preusser, F. (2001). Lumineszenzalter von Quartärablagerungen im Donautal und im Tertiärhügelland bei Ingolstadt Bayern. *Geologica Bavarica*, **106**: 259-271.

Fiebig, M. and Preusser, F. (2003). Das Alter fluvialer Ablagerungen aus der Region Ingolstadt (Bayern) und ihre Bedeutung für die Eiszeitenchronologie des Alpenvorlandes. Zeitschrift für Geomorphologie NF. (in press)

Fuchs, M. and Lang, A. (2001). OSL dating of coarse-grain fluvial quartz using single-aliquot protocols on sediments from NE Peloponnese, Greece. *Quaternary Science Reviews*, **20**: 783-787.

Fuller, I.C., Wintle, A.G. and Duller, G.A.T. (1994). Test of partial bleach methodology as applied to the infra-red stimulated luminescence of an alluvial sediment from the Danube. *Radiation Measurements*, **23**: 539-544.

Geyh, M.A. and Schlüchter, Ch. (1998). Calibration of the ^{14}C time scale beyond 22,000 BP. *Radiocarbon*, **40**: 475-482.

Hilgers, A., Murray, A., Schlaak, N. and Radtke, U. (2001). Comparison of quartz OSL protocols using Lateglacial and Holocene dune sands from Brandenburg, Germany. *Quaternary Science Reviews*, **20**: 731-736.

Hormes, A., Preusser, F., Denton, G., Hajdas, I., Stocker, T. and Schlüchter, Ch. (2003). Radiocarbon and luminescence dating of overbank deposits intercalating outwash sediments of the LGM in North Westland, New Zealand. *New Zealand Journal of Geology and Geophysics*, **46**: 95-106.

Huntley, D.J. and Baril, M.R. (1997). The K content of the K-feldspars being measured in optical and thermoluminescence dating. *Ancient TL*, **15**: 11-13.

Jerz, H. and Mangelsdorf, J. (1989). Die interglazialen Kalksinterablagerungen bei Hurlach nördlich Landsberg am Lech. *Eiszeitalter und Gegenwart*, **39**: 29-32.

Kitagawa, H. and van der Plicht, J. (1998). A 40,000-year varve chronology from Lake Suigetsu, Japan: Extension of the ^{14}C calibration curve. *Radiocarbon*, **40**: 505-515.

Kovanda, J. (1989). Fossile Mollusken in Kalksinterablagerungen (Dauchen) am Lech-Ufer östlich Hurlach (nördlich Landsberg/Lech). *Eiszeitalter und Gegenwart*, **39**: 33-41.

Krbetschek, M.R., Götze, J., Dietrich, A. and Trautmann, T. (1997). Spectral information from minerals relevant for luminescence dating. *Radiation Measurements*, **27**: 695-748.

Murray, A.S. and Wintle, A.G. (2000). Luminescence dating of quartz using an improved single-aliquot regenerative-dose protocol. *Radiation Measurements*, **32**: 57-73.

Preusser, F. (1999a). Lumineszenzdatierung fluviatiler Sedimente - Fallbeispiele aus der Schweiz und Norddeutschland. *Kölner Forum für Geologie und Paläontologie*, **3**: 1-62.

Preusser, F. (1999b). Luminescence dating of fluvial sediments and overbank deposits from Gossau, Switzerland: Fine grain dating. *Quaternary Geochronology (Quaternary Science Reviews)*, **18**: 217-222.

Preusser, F., Geyh., M.A. and Schlüchter, Ch. (2003). Timing of late-Pleistocene climate change in lowland Switzerland. *Quaternary Science Reviews*, **22**: 000-000. (in press)

Preusser, F. and Kasper, H.U. (2001). Comparison of dose rate determination using high-resolution gamma spectrometry and inductively coupled plasma - mass spectrometry. *Ancient TL*, **19**: 19-23.

Rees-Jones, J. and Tite, M.S. (1994). Recuperation of IRSL after bleaching and consequences for dating young sediments. *Radiation Measurements*, **23**: 569-574.

Schlüchter, Ch., Maisch, M., Suter, J., Fitze, P., Keller, W.A., Burga, C.A. and Wynistorf, E. (1987). Das Schieferkohlenprofil von Gossau (Kanton Zürich) und seine stratigraphische Stellung innerhalb der letzten Eiszeit. *Vierteljahrsschrift der Naturforschenden Gesellschaft Zürich*, **132**: 135-174.

Stokes, S., Colls, A.E.L., Fattahi, M. and Rich, J. (2000). Investigation of the performance of quartz single aliquot D_E determination procedures. *Radiation Measurements*, **32**: 585-594.

Visocekas, R. and Zink, A. (1999). Use of the far red TL emission band of alkali feldspars for dosimetry and dating. *Quaternary Geochronology (Quaternary Science Reviews)*, **18**: 271-278.

Wallinga, J., Murray, A.S and Duller, G.A.T. (2000a). Underestimation of equivalent dose in single-aliquot optical dating of feldspars caused by preheating. *Radiation Measurements*, **32**: 691-695.

Wallinga, J., Murray, A.S. and Wintle, A.G. (2000b). The single-aliquot regenerative-dose (SAR) protocol applied to coarse-grain feldspar. *Radiation Measurements*, **32**: 529-533.

Wallinga, J., Murray, A.S., Duller, G.A.T. and Törnqvist, T.E. (2001). Testing optically stimulated luminescence dating of sand-sized quartz and feldspar from fluvial deposits. *Earth and Planetary Science Letter*, **193**: 617-630.

Wallinga, J. (2002). On the detection of OSL age overestimation using single-aliquots techniques. *Geochronometria*, **21**: 17-26.

Wallinga J., Murray A.S. and Botter-Jensen L. (2002). Measurement of the dose in quartz in the presence of feldspar contamination. *Radiation Protection Dosimetry*, **101**: 367-370.

Wintle. A.G. (1973). Anomalous fading of TL in mineral samples. *Nature*, **245**: 143-144.

Reviewer

G. Duller

Comments

The reliability of luminescence ages based on feldspars continues to be a source of debate. The paper by Wallinga et al. (2001) contains compelling evidence to suggest that, at least for the sites that they studied, feldspars are not a reliable chronometer. However, experience elsewhere suggests that some feldspar ages are accurate. The dilemma we then face is how to determine whether a feldspar age is reliable when no independent chronology is available. This paper by Preusser is important firstly in providing further evidence that some feldspar ages are reliable, and secondly in giving a number of suggestions for tests that can be undertaken to assess the quality of the ages produced.

Photomultiplier and filter combinations for the detection of relatively long wavelength (λ>600 nm) luminescence emissions from feldspar

Mortezza Fattahi [a,b] and Stephen Stokes [b]

(a) The Institute of Geophysics, Tehran University, Kargar Shomali, Tehran, Iran. (Corresponding author: Fax: 98-21 8009560, or 44-1865271929 Morteza.fattahi@geography.ox.ac.uk)

(b) Oxford Luminescence Research Group, School of Geography and the Environment, University of Oxford, Mansfield Road, Oxford OX1 3TB.

(Received 15 January 2003)

***Abstract** : We describe our efforts to detect IR-stimulated (λ ~ 833nm) orange-red emission ($\lambda_{emission}$ = 600-750 nm) luminescence from potassium feldspars for dating applications. The aim here is to provide basic information about the detection of orange-red IRSL, as an alternative to conventional IRSL approaches which typically exploits portions of the IR-stimulated UV-blue ($\lambda_{emission}$ < 600 nm) luminescence. We describe modifications to a standard Risø reader, which make it possible to detect orange-red IRSL. Modification consist of various optical filter combinations and extended range, cooled photomultipliers. The use of a modified Electron Tubes D716A "green" bialkaline PMT (green tube) provides a greater quantum efficiency (0.1- ~5% QE) in the wavelength range 600-700 nm than the traditionally used 9635 bialkaline tube (1-negligible% QE @ 600-700 nm). An extended S20 9650 PMT (red tube) provides a greater quantum efficiency (~7-12% QE) in the wavelength range 600-700 nm than both the 9635 and D716A. A substantial disadvantage of using an extended S20 tube is its relatively high quantum efficiency (2.5%) at 830 nm. Filter combinations were examined by both a UV-visible spectrometer and direct measurement of filter/PMT transmission characteristics. Our data suggest that optimal PMT/filter combinations consist of using the green PMT + two FR 400S + BG 39 and either OG 590 or RG 665 for detection of either a broad orange-red (λ ~ 600-720 nm) or far red (λ ~ 670-720 nm), respectively. The green PMT and an Omega 625DF 50 filter is the optimal combination for orange-near red (600-660 nm) emission.*

Introduction

There are potential advantages in using feldspars for luminescence dating of geological and archaeological deposits. These include, the potential for dating over a wide time range; the relatively high luminescence sensitivity to dose; ease of light collection (relating to the wide separation of stimulation and emission bands in conventional IRSL methods); and the significant internal dose of K-feldspars in many cases reducing the uncertainty in measurements of dose rate (Duller, 1997; Fattahi and Stokes, 2001). Wintle (1973) was the first to used feldspar as a natural integrated dosimeter. She observed significant age underestimation and attributed it to the phenomenon of "anomalous fading", where the observed signal stability is far lower than that predicted from kinetic analyses.

Anomalous fading has significantly hindered the use of feldspars in luminescence dating through the loss of stored charge (Visocekas and Zink, 1999; Huntley and Lamothe, 2001). This has resulted in severe age underestimations in many dating applications and a number of approaches have been proposed to circumvent this effect (For review see Fattahi and Stokes, 2002a). One of these approaches is to look for a non-fading signal. Zink and Visocekas (1997) reported that two TL emission bands in feldspar, one in the blue range and another in the far-red, could be separated, below and above 600 nm (Figure 1). The two bands exhibited similar trap activation energies, dose variation and bleaching characteristics, but different in terms of their kinetic and glow peak temperatures. In particular, the red emission band appeared to be unaffected by anomalous fading, and was therefore considered more suitable for dating (Zink and Visocekas, 1997). Zink and Visocekas (1997) successfully dated three feldspars of volcanic origin using the far-red TL emission alone with an additive-dose protocol.

Red TL of feldspar is optically bleachable (e.g., Bos et al., 1994; Prescott et al., 1994; Zink and Visocekas, 1997). Bos et al. (1994) reported a more intense red (at λ ~ 730 nm) than blue emission in oligoclase. They showed that artificially irradiated oligoclase was bleachable, and that the bleaching efficiency of both the blue and red emissions increased with decreasing wavelength. While the sample remained unbleached at wavelengths between 703-800 nm. However, they made no study of the effect of stimulating wavelengths exceeding 800 nm, the

wavelengths currently used for IRSL. Prescott et al. (1994) reported that sunlight bleaches red emissions (>650 nm) of TL in some feldspars. Zink and Visocekas (1997) observed that the shorter sunlight wavelengths, around 350-400 nm, showed a higher bleaching efficiency with similar bleaching results in both bands.

None of the above workers explored the effect of IR (λ > c. 800nm) exposure on red luminescence emissions. However, since there is sufficient information on the similarity of trapping centres involved in the blue and red emissions (e.g., Bos et al., 1994; Zink and Visocekas, 1997), it can be assumed that IRSL using feldspar's red emissions may be useful for dating applications. Optically-stimulated red luminescence (including visible and IR stimulation) could provide methods for the exploitation of feldspars in dating applications provided that the technological problems in its detection, including the effect of black body radiation and fluorescence, can be overcome.

Given its potential to circumvent anomalous fading, we consider the development of a suitable detection system and the testing of IR stimulated red emission to be a key priority in luminescence dating and one which we have begun to evaluate. As with conventional OSL of quartz and IRSL of feldspars, practical advantages in exploiting anti-Stokes radiation encouraged us, in combination with the well-known feldspar stimulation IR resonance, to first consider the use of IR stimulation wavelengths to detect a red emission. As the initial TL investigations in this area (e.g., Zink and Visocekas, 1997) studied orange-red TL (λ c. 600 - 750 nm) to overcome anomalous fading, we decided to similarly investigate an orange-red IRSL signal with same wavelength range.

This paper is a companion of another paper (Fattahi and Stokes, 2002b) which presents the first contribution for exploring the suitability of the orange-red IRSL of feldspar for dating applications.

Our aim here is to describe our attempts to assemble and test apparatus to detect orange-red IRSL and TL from feldspar, including an overview of the photomultiplier and filter combinations which we have tested.

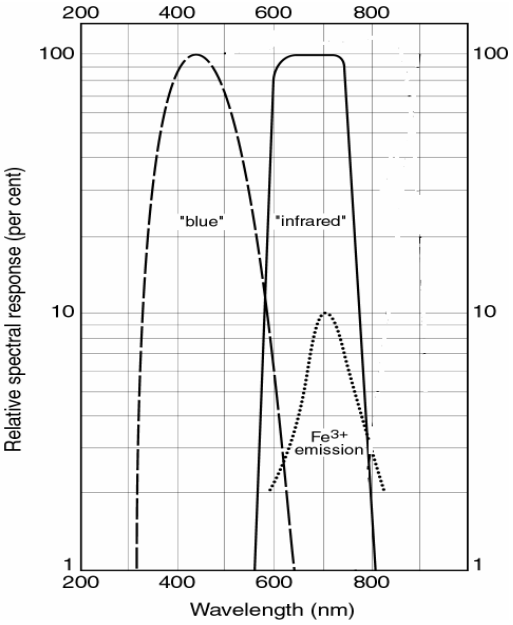

Figure 1.
Blue and IR band for feldspar (modified from Zink and Visocekas, 1997). Continuous line: normalized spectral responses of the arrangements for detection and filtering of the two TL emission bands; IR, with an AsGa photocathode (C 31034 PMT), and two filters (Schott OG 590 + Corion LS 750); Blue with a bialkali photocathode (EMI 9924 PMT) and a filter (Schott BG 18). Short-dashed line: Fe^{3+} emission in feldspar.

2. The photo-detection system

Photomultiplier tubes (PMT)

To increase the detection efficiency of red signal and decrease the IR background, a suitable photo detection system must be employed that detects red wavelengths between 600-750 nm, and cuts the IR wavelengths greater than 750 nm. There is no ideal PMT with high quantum efficiency at red emission and 0% QE at other wavelengths. Figure 2a shows the spectral response and quantum efficiency of selected widely available photomultiplier tubes.

While bialkaline PMTs, such as the Electron Tubes 9635Q "blue" tube, are highly suited to the detecting of UV-blue emission, they have poor quantum efficiency at longer wavelengths (Figure 2a). As can be seen in Figure 2a, the 9635Q photocathode should not be sensitive to wavelengths greater than c. 650 nm, which potentially is a great advantage for

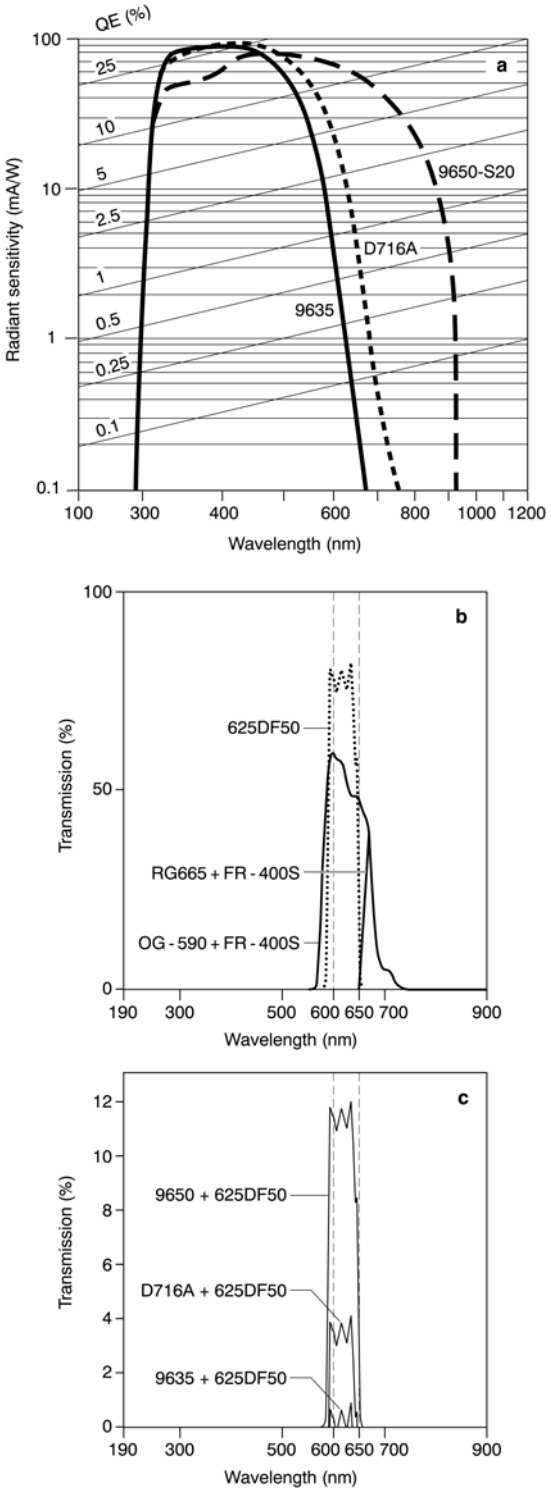

Figure 2.
The expected red detection window through different PMTs and filters. (a) PMT quantum efficiencies. (b) The transmission characteristics of Omega 625 DF50 filter and either a combinations of an FR 400S and either OG590 or RG 665 filters. (c) Transmission window resulting from a combination of Omega 625 DF50 and the PMTs.

preventing background produced in the IR range. However, in empirical tests we have found that this PMT is significantly sensitive to IR, which may be due to photosensitivity in the coating of the first dynode (Aitken, 1998). The limited IR sensitivity of a 9635Q type PMT has actually been noted and exploited by other workers (e.g. Miallier et al., 1991).

The use of an extended S20 9650 PMT (red tube) provides a greater quantum efficiency (15% QE) in the wavelength range 600-700 nm than the traditionally used 9635 bialkaline tube (0.1% QE @ 600-700 nm). This red high sensitivity tube is particularly suitable for the detection of red thermoluminescence and has been successfully employed in RTL studies (Fattahi and Stokes, 2000a, b). A substantial disadvantage of using such an extended S20 tube is its relatively high quantum efficiency (2.5%) at 830 nm (the IR laser diode peak emission wavelength in our RISO reader [Boetter-Jensen et al., 2000]) and high dark count at room temperature (c. 2,000 $c.s^{-1}$). While this thermally-generated dark count can be reduced by an order of magnitude by active cooling down to c. -15°C (Fattahi and Stokes 2000a: Figure 3), the sensitivity of the tubes at the IR stimulation wavelength remains problematic. There are two obvious alternative approaches. Firstly, to use an IR laser source with a wavelength peak at greater wavelength (i.e. $\lambda > 950$ nm). Such a wavelength is within the IR stimulation spectrum of feldspars (Spooner and Franks, 1990; Duller, 1997), but should not be detected by an S20 9650 PMT (Figure 2). However, it should be noted that Figure 2a shows almost no sensitivity for blue PMT at 830 nm, while empirical tests have demonstrated this not to be the case. On this basis some IR sensitivity might be anticipated for the red PMT even at 1000 nm. A second option would be to exploit a PMT with a spectral response greater than that of the "blue" tube, but less extended than the "red" S20 tube. This second option was pursued and a "green" PMT (EMI D716A) was tested. The advantages and limitations of these three available PMTs that can be used for orange-red IRSL studies are summarized in Table 1.

We have attached a D716A PMT to a Risø model TA-15a automated TL/OSL reader using a flange that locates the D716A tube above the standard Risø OSL/IRSL collar. This arrangement allows routine operation of the Risø reader while either the 'red' or 'green' 'blue' tube is mounted. This flange is similar to the flange used for locating the S20 PMT above the Risø reader (Fattahi and Stokes, 2000a, Figure 2) but with reduced height (16 mm in comparison to 43 mm for the original collar which was designed to incorporate an optical fiber input), which increases the photon yield.

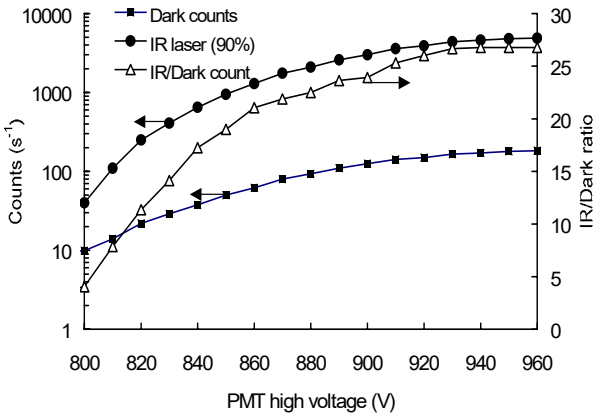

Figure 3.
The voltage dependent response of EMI bialkaline D716A "green" tube. A blank stainless steel disk was used to measure the reflection of IR.

Similarly to the S-20 PMT, a disadvantage of the D716A PMT is its relatively high dark count at room temperature (c. 2,000 $c.s^{-1}$). This thermally-generated dark count can be reduced by an order of magnitude to levels comparable to that of a 9635 bialkali tube by active cooling down to ~ -20°C. For this purpose we use the same Thermoelectric Refrigerated Chamber as described earlier. Maximum cooling (~Δ40°C) can be achieved within 1 hour of switching on, while the warm-up cycle takes on the order of 3 hours. We tested the voltage response of the D716A PMT and found its response characteristics and optimised voltage to be similar to that for conventionally used 'blue' tubes (Figure 3).

Optical filters

In considering filter combinations for orange and red emission IRSL measurements, we attempted initially to maximize luminescence transmission of 600-750 nm, while minimizing passage of other photons. The main reason for choosing 600 nm as the lower wavelength bound of the transmission window is the success of Zink and Visocekas (1997) who overcome anomalous fading in TL from feldspar using a similar transmission window and a Schott OG590 orange-red transmission filter. In subsequent experiments we have attempted to identify filter combinations, which isolate far red (i.e. λ >665 nm) emissions. We have tested a range of filter combinations by measuring transmission windows using a UV-IR spectrophotometer. Six heat (IR) rejection filters were incorporated in our tests (Figure 4a). The filters tested consist of both those, which are widely available and in use in luminescence laboratories, and a series of relatively new multilayer varieties. The Hoya HA-3 and Schott BG-39 are widely employed in TL and OSL applications for long cut filtering and heat rejection (Aitken, 1998). We additionally tested a multi-layer laminated Corion FR-400S, a Delta SWP 685, and an Omega 750 SP interference filter (Figure 4). There are ranges of long pass filters capable of restricting wavelengths shorter than c. 600nm. Of these we have chosen to examine the characteristics of the Schott OG-590 [the filter employed by Zink and Visocekas (1997)] and Schott RG-665 filters. Additionally, a band pass Omega 625DF50 filter has been tested to observe orange-near red (λ c. 600-660 nm) emissions (Figure 2b).

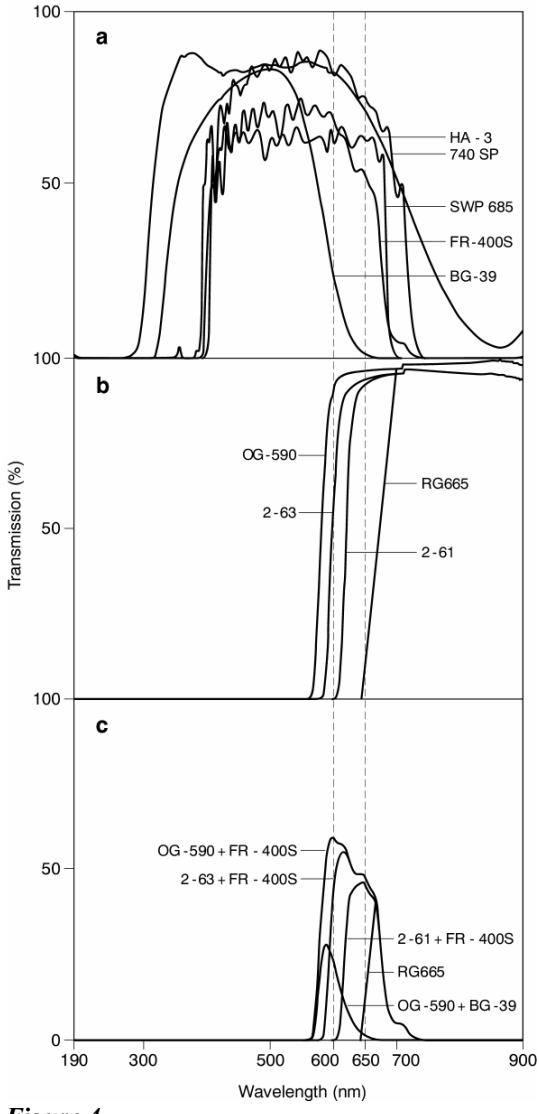

Figure 4.
Transmission characteristics of selected (a) long cut filters, (b) short cut filters and (c) the combination of some long and short cut filters.Spectrophotometer analysis

All spectrophotometer measurements were undertaken at room temperature using a Shimadzu UV-IR spectrophotometer model P/N 204-58000. Examination of the long cut filters characteristics reveals strong contrasts (Table 2). While the HA-3 filter offers a broad transmission window passing from UV to red at levels in excess of 60%, its high (20%) transmission in to the IR renders it of limited utility for RTL and orange-red IRSL studies. Detailed examination of the Schott BG-39; Corion FR 400S; Delta SWP BL 685 and Omega 625DF50 transmission characteristics reveal minor but important IR pass windows at around 760-900 nm (Table 2). While the high signal pass levels are advantageous in red luminescence studies, these IR pass windows significantly complicate sample stimulation with IR.

Of the filters tested the BG-39, Corion FR 400S, Delta SWP BL 685 and Omega 625DF50 offer the best (i.e., lowest) IR transmission characteristics between 760-900 nm. However, the BG-39 transmits only c. 20% of that passed by the FR-400S in the wavelength region 600-700 nm. The Omega 625DF50 transmits 80% of the signal between 600-640 nm and c. 60% transmission between 640-660 nm. Omega 740 SD offers the highest transmission between 600-700 nm (>60%), but it is an inefficient heat rejection filter with ~1.1% transmission between 890-900 nm (Table 2). None of the IR cut filters examined fully cuts unwanted low energy photons (>750 nm) and pass all signals between 600-750 nm. As an alternative, we have explored combinations of long cut filters.

The results for selected filter combinations are summarized in Figure 4. Of these, the combination of FR-400S plus OG-590 and Omega 625DF50 alone, provide the greatest red signal transmission, while decreasing the spectral range of transmission, to levels lower than c. 730 nm and c. 670 nm, respectively (Table 3). We note additionally, that in testing for phosphorescence or other malign effects, the orientation or ordering of the filters had no observed effect on the transmission windows.

To demonstrate the combined effect of photomultiplier tubes and filter transmissions, the estimated quantum efficiencies (QE) for the PMTs of Figure 2a have been used. The QE at maximum wavelength for EMI 9635 PMT is 0.1% at 620 nm. Therefore, the effect of PMT quantum efficiency (QE) on signal transmission has been estimated, based on their efficiency at 620 nm, rather than at 710 nm or individual wavelengths. The estimated quantum efficiencies for the PMTs at 620 nm are ~ 0.1, 5 and 15% for the blue, green and red PMT's, respectively. As an example, the expected detection windows and intensities for the combination of Omega 625 DF50 and the three photomultipliers tested in this study are displayed in Figure 2c. A more detailed investigation is required to precisely quantify details of the transmission windows.

.

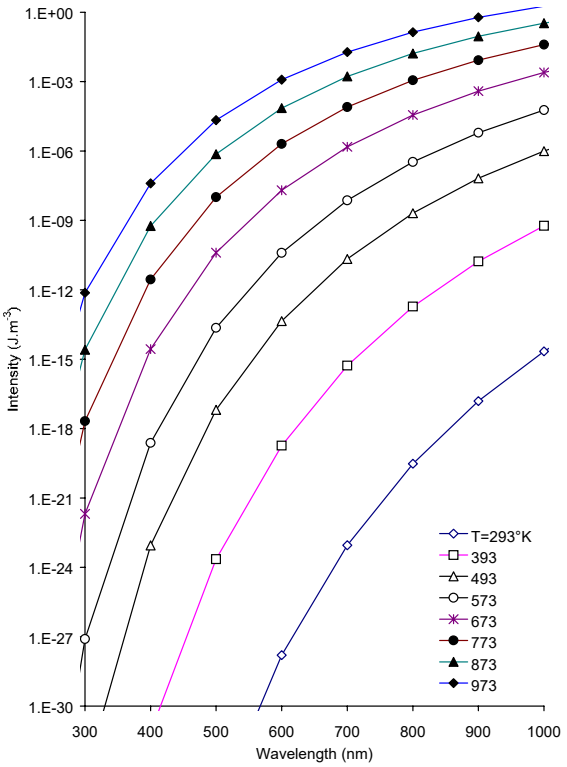

Figure 5.
Black body radiation obtained using Planck's law. The emission intensity of blackbody radiation plotted versus different wavelengths at temperatures shown.

Actual orange-red IRSL measurements using various filter and PMT combinations

In IRSL, the stimulation is generally thought to be a thermally–assisted photon process (Hütt et al., 1988). Increasing the sample temperature will increase the signal (Aitken, 1998). While increasing the sample temperature (for preheating or stimulation) has advantages including increasing the IRSL signal, it has a potential disadvantage of thermal incandescence. Thermal incandescence has previously hampered the application of red emission in thermoluminescence dating (e.g. Fattahi and Stokes, 2002a). Figure 5 shows the theoretical black body curves calculated from Planck's law. As can be seen in Figure 5, black body radiation increases with both substrate temperature and radiation wavelengths from 200 to 900 nm. The highest intensity of thermal incandescence (c. 10^{-2} J.m^{-3}) in TL studies will appear at ~ 500°C at 900 nm. In comparison, the intensity of typical 1W solid state infrared (830 ± 5 nm) laser

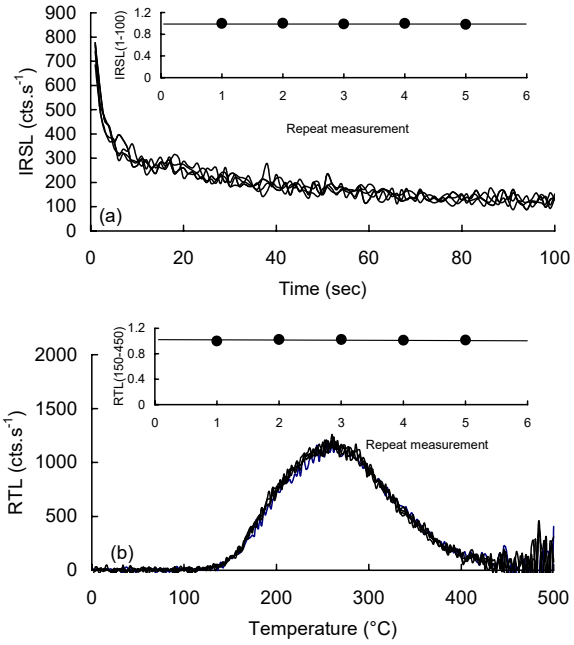

Figure 6.
*Orange-red IRSL and RTL reproducibility plot (from Fattahi and Stokes, 2002b). Orange-red IRSL and RTL of feldspar sample (lab No. 99/5/1 KF) was measured, respectively after giving a dose of ~ 1200 Gy. The procedure was repeated 5 times. (a) Repeated orange-red IRSL decay curves; inset shows total light sum of IRSL (0-100 sec) from individual curves versus measurement number. (b) Repeated RTL glow curves; inset shows total light sum of RTL (0-500°C) from individual curves versus measurement number. The detection system was EMI 9658 "red" PMT and OG 590 + FR 400S + 2*BG 39 filters*

diode unit is 400 mW.cm^{-2} (Bötter-Jensen et al., 2000). These data suggest that the effect of IR reflection originating from the IR source will be an order of magnitude greater than the effect of thermal incandescence as a background component.

To explore the effect of IR laser diode intensity on background, Fattahi and Stokes (2002b) examined a blank stainless steel disk while varying the laser intensity (0-100%). They demonstrated that there is a significant IR intensity-related background signal. While it is possible to minimize background generated thermally, a major problem is the transmission of the IR stimulation wavelength reflection from the sample.

To confirm the general patterns noted above we tested a range of filter combinations and PMT's using a potassium feldspar sample collected from a New Zealand Ignimbrite (sample 99/5/1) ***(Figure 6, Table 4).*** The sample was repeatedly given a 1200 Gy test dose and its orange-red IRSL and TL, respectively were measured, for a range of filter and PMT combinations (Fattahi and Stokes, 2002b). Orange-red IRSL measurements were made at 75°C for duration of 100 sec using IR intensity.

While there is at present no definitive choice, we consider the green PMT in combination with two FR 400S + BG 39 (1mm) plus OG 590 or RG 665 as an efficient arrangement for detecting the initial rapidly depleting portion of orange-red IRSL decay curves in either a broad orange-red (λ c. >600-720 nm) or far red (λ c. 665-720 nm) emissions, respectively. An Omega 625DF50 in combination with the green PMT is suitable in cases where details of the entire decay form and low background levels are required in near red (λ c. 600-660 nm) part of the spectrum. Alternatively, for very bright samples if neither the red or green PMT are available, an Omega 625DF50 or BG 39 + OG590 filters combined with a blue PMT may provide a usable combination for near red part of the spectrum. While this would result in a very low signal yield, it has the added advantage of not requiring active cooling.

Conclusion

Orange-red IRSL from feldspar is a potentially useful dosimeter for dating applications. We have evaluated a series of PMT and filter combinations to maximise orange-red IRSL measurements. We have modified a Risø model TA-15 automated TL/OSL reader. Modification consisted of two alternatives cooled PMT and a range of filter combinations which have not previously been employed in optical dating. Using either a cooled (~-20°C) extended Electron Tubes PMT S20, 9658 ("red") or an Electron Tube bialkaline, D716A PMT ("green") provides greater quantum efficiency in the red portion of the spectrum (600-750 nm) than a conventional blue-sensitive, 9635 bialkali PMT. A substantial disadvantage of using these 'red' and 'green' photomultiplier tubes however, is their relatively high quantum efficiency in the infrared. As a result, selection of a suitable filter combination is critical. There is strong evidence that the background is mainly due to the reflection of incident light, which is itself related to the intensity of IR from the IR laser diode (λ = 830 nm). To overcome the high background, we have attached and tested a variety of filter combinations. They included most of the available long cut filters and some long pass filters and one band pass filter. While, this reduces the transmission of IR to a low level, the red signal transmission also decreases. While all these PMTs are capable of measuring an orange-red IRSL signal, our data suggest that optimal

PMT	Limitation	Advantages
Blue: (Electron Tube 9635, bialkaline)	Low QE at red (0.1% at 630 nm)	Low QE at IR (<0.01% at 830nm)
Green: (Electron Tube D716A, bialkaline)	Med QE at red (2.5% at 630 nm) High Dark Noise (2000 $c.s^{-1}$ at room temperature) - requires active cooling to decrease the Dark Noise one order of magnitude (~180 $c.s^{-1}$).	Med QE at IR (0.01% at 830 nm)
Red: (Electron Tube 9650, S20)	High QE at IR (2.5% at 830 nm) High Dark noise (2000 $c.s^{-1}$ at room temperature) - requires active cooling to decrease the Dark Noise one order of magnitude (~200 $c.s^{-1}$).	High QE at red (15% at 630 nm)

Table 1.
Summary characteristics of the three-photomultiplier tubes used for detecting orange- red IRSL (λ c. 600-750 nm).

Filter type and thickness (mm)	Peak Transmission		IR Transmission		Heat and IR Rejection
	%	λ (nm)	%	λ(nm)	
Hoya HA-3 (3)	~ 80	340-620	>20	700->900	Poor
Schott BG-39 (2)	~ 80 ~ 60 ~ 30 ~ 8	450-530 540-580 580-620 620-640	~ 0.2	760-900	Good
Schott BG-39 (1)	~ 40 ~ 30 ~ 15	400-580 580-620 620-660	~ 0.5 ~ 0.1 ~ 0.1	700-720 720-760 860-900	Good
Corion FR – 400S (7)	~ 70 ~ 60 ~ 10	440-600 600-640 680-700	~ 2.0 ~ 0.5 ~ 0.3	700-720 720-740 760-900	Good
Omega 740 SP (2)	~ 85 ~ 80 ~ 60 ~ 20	510-580 460-625 420-680 410-720	~ 0.2 ~ 0.1 ~ 0.6 ~ 1.1	720-760 850-870 870-890 890-900	Medium
Delta SWP BL 685 (2)	~ 65 ~ 35 ~ 10	430-660 400-680 395-690	~ 0.1 ~ 0.1 ~ 0.3	700-750 850-880 880-900	Good
Omega 625DF50 (5)	~ 80 ~ 60 ~ 30	600-640 640-650 650-660	~ 0.1 ~ 0.2	860-880 880-900	Good

Table 2.
Spectral characteristics of some long cut filters

Filters	Max Peak Transmission		Min-Max Wavelength
	%	λ (nm)	λ (nm)
FR-400S + OG-590	60	600-620	570-730
FR-400S + 2-63	52	610-630	580-730
FR-400S +2-61	46	630-650	600-730
FR-400S +3-67	46	570-620	550-730
FR-400S + RG 610	44	620-640	590-730
FR-400S + RG 665	25	670-680	645-730
BG-39 + OG-590	34	590-610	570-720
BG-39 +2-63	29	600-620	580-720
BG-39 +2-61	18	620-640	600-720
HA-3 + OG-590	60	610-630	530-900
BG-39 + RG 610	12	610-630	590-720
BG-39(1)+HA-3 + OG-590	20	580-600	560-720
BG-39(2)+HA-3 + OG-590	21	580-600	560-670
BG-39(1) + HA-3 + 2-63	12	600-620	580-710
BG-39(2) + HA-3 + 2-63	16	600-620	580-670
BG-39(1) + HA-3 + 2-61	8	620-640	600-710
BG-39(2) + HA-3 + 2-61	3	620-630	610-670
BG-39(1)+FR-400S+OG590	14	590-610	570-680
BG-39(2)+FR-400S+OG590	19	580-600	560-770
Omega 625DF50 (5)	80	600-640	590-660

Table 3.

Spectral characteristic of selected filters combination

Filter Combination	PMT	Blank SS BG at 90%	Back-ground (BG)	Signal (S)	S/N	Error S/N	S-BG
HA3+OG590	Blue	2 000.0					
SWP+OG590	Blue	30.0	70.4	91.1	1.29	±0.15	20.7
OM+OG 590	Blue	0.7	0.9	3.1	3.46	±1.11	2.2
FR+OG590	Blue	9.7	7.9	13.2	1.66	±0.33	5.2
BG39(2)+OG590	Blue	0.2	0.2	0.3	1.28	±0.64	0.1
OMEGA 625	Blue	0.7	0.7	2.5	3.80	±1.30	1.9
FR+FR+OG590+BG 39(1)	Blue	0.2	0.2	0.2	1.18	±0.65	0.0
SWP+OG590	Green	64.0	125.7	147.2	1.17	±0.12	21.5
OM+OG 590	Green	8.2	14.2	17.2	1.21	±0.22	3.0
FR+OG590	Green	8.0	11.9	15.4	1.30	±0.24	3.5
BG39(2)+OG590	Green	0.2	0.2	1.3	5.43	±2.33	1.1
OMEGA 625	Green	0.4	0.6	3.3	5.35	±1.82	2.7
BG39(1)+OG590	Green	2.4	3.2	5.6	1.75	±0.44	2.4
FR+FR+OG590	Green	0.5	0.7	3.0	4.45	±1.50	2.3
OM+FR+OG590	Green	0.0	1.4	4.0	2.79	±0.81	2.6
FR+Delta+OG 590	Green	0.4	0.4	1.3	2.96	±1.15	0.9
FR+ BG39(2)+OG 590	Green	0.2	0.2	1.1	4.71	±2.08	0.8
FR+FR+BG 39(1)+OG590	Green	0.2	0.3	1.6	4.76	±1.90	1.3
OM+FR+OG590	Red	110.0	123.3	142.8	1.16	±0.12	19.5
OM+FR+OMEGA 625	Red	3.0	29.3	33.6	1.15	±0.17	4.3
FR+BG39(2)+OG590	Red	3.0	3.1	8.5	2.78	±0.67	5.4
FR+BG39(1)+OG590	Red	50.0	43.6	63.0	1.44	±0.19	19.4
FR+FR+BG39(1)+OG590	Red	0.4	4.7	15.5	3.30	±0.70	10.8
BG39(1)+BG39(2)+ OG590	Red	11.0	10.3	14.6	1.42	±0.27	4.3
FR+BG39(1)+BG39(2)+ OG590	Red	0.4	0.5	1.2	2.29	±0.88	0.6

SWP = DELTA SWP 685 (18 mm dia); OM = Omega 750 SP; FR = Corion FR 400 S.

The units of ginal and background are counts per second (cts.s^{-1}) and shown by (kcts.s^{-1})

Table 4.
Selected combinations of different filters and three blue, green and red PMTs (from Fattahi and Stokes, 2002b).

PMT/filter combination consist of either the green PMT + two FR 400S + BG 39 and OG 590 or RG 665 for wide red (600-720 nm) or far red (670-720 nm), respectively. The green PMT and an Omega 625DF 50 filter is the optimal combination for near red (λ c. 600-660 nm) emissions.

Aknowledgements

Ministry of Science, Research and Technology of Iran and Tehran University kindly supported funding of MF. Particular thanks are due to Ailsa Allen and David Sansom for technical support. We gratefully acknowledge Mike Homer and his colleagues (Electron Tube Limited) for providing the D716A PMT and technical support. The authors would like to thank Professor Michel Lamothe and Professor John Prescott for their ongoing advice. MF gratefully acknowledges Mrs G. Fattahi for general support.

References

Aitken M. J. 1998 An Introduction to Optical Dating: The dating of Quaternary sediments by the use of photon-stimulated luminescence. Oxford University Press. 267 pp.

Bos, A.J.J., Piters, T.M. and Ypma, P.J., 1994. Thermoluminescence emission spectra and optical bleaching of oligoclase. Radiation Measurements, 23: 349-353.

Bøtter-Jensen L., 1997. Luminescence techniques: instrumentation and methods. In Luminescence and ESR dating and allied research. Radiation Measurements (ed. A. G. Wintle), 27, 749-768. Pergamon.

Bøtter-Jensen L., Bulur, E. Duller, G. A. T. and Murray, A. S., 2000. Advances in luminescence instrument systems, Radiation Measurements, 32, (5-6), 523-528

Duller G. A. T., 1997. Behavioural studies of stimulated luminescence from feldspars. Radiation Measurements 27, 663-694.

Fattahi M. and Stokes S., 2000a. Red thermoluminescence (RTL) in volcanic quartz: development of a high sensitivity detection system and some preliminary findings. Ancient TL 18, 35-44.

Fattahi M. and Stokes S., 2000b. Extending the time range of luminescence dating using red TL (RTL) from volcanic quartz. Radiation Measurements 32, 479-485.

Fattahi, M., 2001. Studies on red thermoluminescence and infrared stimulated red luminescence. Unpublished D. Phil. thesis, Oxford University, Oxford.

Fattahi M. and Stokes S., 2001. Luminescence dating of Quaternary Volcanic events. A review of previous investigations and some observations on the potential of red luminescence emissions. School of Geography of university of Oxford Research papers, 58, 1-72

Fattahi M. and Stokes S., 2002a. Dating volcanic events by luminescence. Earth science review. In press.

Fattahi M. and Stokes S., 2002b. Infrared stimulated red luminescence from potassium feldspar for dating applications. Radiation Measurements. accepted.

Huntley D. J. and Lamothe M., 2001. Ubiquity of anomalous fading in K - feldspar and the measurement and correction for it in optical dating. Canadian Journal of Earth Sciences 38, 1093-1106.

Hütt G., Jaek I., and Tchonka J., 1988. Optical dating: potassium feldspars optical response stimulation spectra. Quaternary Science Reviews 7, 381-385.

Miallier, D. et al., 1991. Properties of the red TL peak of quartz relevant to thermoluminescence dating. Nuclear Tracks and Radiation Measurements, 18(1/2): 89-94.

Prescott, J.R., Fox, P.J., Robertson, G.B. and Hutton, J. T., 1994. Three-dimensional spectral studies of the bleaching of the thermoluminescence of feldspars. *Radiation Measurements*, 23(2-3): 367-375.

Spooner, N.A. and Franks, M., 1990. Some characteristics of infrared emitting diodes relevant to luminescence dating. Ancient TL, 8: 16-19.

Visocekas, R. and Zink, A., 1999. Use of the far red TL emission band of alkali feldspars for dosimetry and dating. *Quaternary Science Reviews (Quaternary Geochronology)*, 18: 271-278.

Wintle, A.G., 1973. Anomalous fading of thermoluminescence in mineral samples. *Nature*, 245(5421): 143-144.

Zink A. J. C. and Visocekas R., 1997. Datability of sanidine feldspars using the near-infrared TL emission. Radiation Measurements 27(2), 251-261.

Reviewer

D. Miallier

IRSAR – A single-aliquot regenerative-dose dating protocol applied to the infrared radiofluorescence (IR-RF) of coarse-grain K-feldspar

G. Erfurt* **and M.R. Krbetschek**
Sächsische Akademie der Wissenschaften zu Leipzig, Quaternary Geochronology Section at Institute of Applied Physics, TU Bergakademie Freiberg, Bernhard-von-Cotta-Str. 4, 09596 Freiberg, Germany
*corresponding author: Gunter Erfurt, Phone +49 3731 392163, Fax +49 3731 39 4004, Email address: gerfurt@physik.tu-freiberg.de

(Received 24 March 2003; in final form 3 April 2003)

Abstract: *Since the infrared radiofluorescence (IR-RF) at 865 nm emitted by potassium-rich feldspars has been proven to be suitable for sediment dating, all instrumentation requirements for this new dating technique have been met. This paper describes the single-aliquot regenerative-dose protocol IRSAR (infrared radiofluorescence single-aliquot regenerative-dose) applied to coarse-grain K-feldspar. Based on state-of-the-art knowledge of the physical background and the methodology, this promising new technique can be used for the dating of clastic sediment samples in the age range up to over 250 ka.*

1. Foreword

The first papers concerning the radiofluorescence of K-feldspar and its potential as a luminescence dating method used the expression "infrared radioluminescence (IR-RL)" (e.g. Trautmann et al. 1999a). In solid state physics literature, the nomenclature for luminescence phenomena refers usually to the fundamental luminescence excitation mechanisms. Whereas "radioluminescence" includes all luminescence effects induced by interaction with ionising radiation, e.g. radiophosphorescence processes like thermoluminescence and optically stimulated luminescence. The phenomenon described in the present paper arises from prompt radiative charge transitions during interaction of the samples with ionising radiation and is, irrevocably, a fluorescence process. Thus to avoid misunderstanding, we suggest the abbreviation "IR-RF" as synonym for the infrared radiofluorescence of K-feldspars

2. Introduction

2.1 Physical background

Radiofluorescence (RF) is a well known phenomenon, which arises from prompt radiative charge transitions during interaction with ionising radiation. Historically, the radiofluorescence of ZnS helped raise Rutherford (1911) to the scientific Pantheon when he used this to determine the scattering of α and β particles in a gold foil to prove the existence of the atomic structure. For radiofluorescence of ZnS the synonym "scintillator" was introduced and this kind of radiofluorescence is still used when NaI:Tl detectors are applied to γ spectrometry tasks.

The present paper describes the radiofluorescence of coarse-grain K-feldspar, for which the experimental set-up, first described by Trautmann et al. (1998), is illustrated in figure 1.

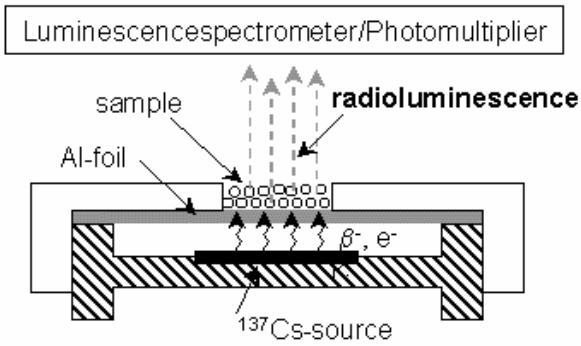

Figure 1.
Schematic of equipment for radiofluorescence measurements using a laboratory β source (after Trautmann et al., 1998)

K-feldspar coarse-grains with a grain size of 130 to150 µm are fixed on an aluminium foil or, as reproducable mono-layers with defined thickness, on thin adhesive foil strips. The laboratory ^{137}Cs source fulfils two tasks: excitation of the fluorescence and the application of a β dose.

The simple two-term energy band model in figure 2 shows the process of prompt radiative charge trapping and recombination which arises from

interaction of K-feldspar with ionising radiation. Electrons (black dots) are excited by ionising radiation and transfer from the valence band (VB) to the conduction band (CB) (transition *a*).

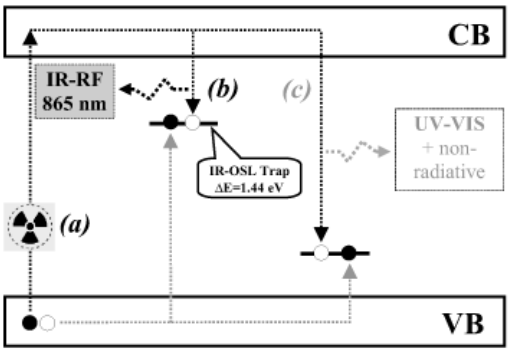

Figure 2.
Simple two-term energy band model which shows the fundamental physical idea behind IR-RF dating, especially the radiative electron transition from the conduction band (CB) to the IR-RF (IR-OSL) trap emitting characteristic fluorescence light at 865 nm.

Electrons thus transferred to the conduction band only remain a few nanoseconds in this delocalised state and immediately are forced to recombine with holes and electrons in the valence band (direct CB→VB transition not shown in the figure). These are attracted to hole traps in the band gap, resulting from the presence of several intrinsic or extrinsic defects, and this leads to recombination at metastable traps or recombination centres (transition *b* and *c*) emitting characteristic fluorescence light. In contrast to other materials, only the types of K-feldspar classified as microcline, orthoclase (and amazonite) show radiofluorescence in the infrared at 865 nm (IR-RF), which is interpreted as radiative electron transition from the conduction band to the trap (transition *b*). In all other feldspars, the transitions from the conduction band to the dosimetric traps are non-radiative and the energies of the electrons are dissipated by phonon processes somewhere in the crystal lattice. Because of the similarity of the IR-OSL excitation energy of 1.44 eV (855 nm) and the wavelength of the IR-RF at 865 nm (1.43 eV), Trautmann et al. (1999a,b) concluded that the IR-RF trap and the IR-OSL trap originate from the same crystalline defect. The other special feature of the IR-RF process is the completely different behaviour of the dose response curve. The IR-RF signal decreases exponentially with given dose and its saturation level is reached after about 1300 Gy dose. This can also be explained using the model in figure 2: The intensity of the IR-RF intensity depends on the electron density in the IR-RF (IR-OSL) trap. The higher the density of trapped electrons, the lower is the probability that other electrons can undergo the transition into this trap; this results in a decrease of the IR-RF intensity. Furthermore, the stability of the dosimetric signal does only depends directly on the thermal behaviour of the IR-RF (IR-OSL) trap. This transition also takes place in the radioactive environment of the K-feldspar crystals in sediments. Therefore, the IR-RF (IR-OSL) trap is filled continuously during burial. The processes in nature and in the laboratory are absolutely comparable, apart from different dose rates. The "radiative" filling of traps continues in the laboratory. Thus measurement of the IR-RF is the first opportunity in luminescence dating to monitor the electron density in a trapping state and to use it as primary dating information.
The electron density in the trap can be altered by sunlight with wavelengths less than 550 nm within about one hour (Trautmann et al. 1999a,b) and by a laboratory solar simulator within a few minutes (Krbetschek et al. 2000). This fulfils the bleaching requirements for sediment dating.

The radiofluorescence signal is not restricted to the infrared. Emissions in the UV-VIS can also be excited (transition *c*) and they are understood to be radiative recombinations into recombination centres during interaction with ionising radiation. With dose, their intensities mostly increase and can be explained in the same way as the decreasing IR-RF intensity: the more traps that are filled with electrons, the higher is the probability for electron recombinations into recombination centres.

Transitions shown in grey for holes (black circles) are needed for charge neutrality in irradiated crystals. During laboratory irradiation, holes will continuously move from the valence band to UV-VIS recombination centre(s) as well as to the IR-RF (IR-OSL) trap. This explains why the IR-RF saturation level shows a constant residual IR-RF signal.
More detailed information about the physical background and modeling approaches of this special luminescence effect are given in the literature review in section 2.2 below.

2.2 Literature review

Trautmann et al. (1998) reported pioneering investigations of spectral and dosimetric radiofluorescence (RF) properties of alkali feldspars, Trautmann et al. (1999a) realised the potential of the dating application of the infrared radiofluorescence (IR-RF) that only occurs in potassium feldspars, such as microcline and orthoclase. The IR-RF was explained as the radiative transition of electrons from the conduction band via the excited state to the ground state of the 1.44 eV IR-OSL trap, emitting

characteristic luminescence at 865 nm. This was inferred from the strict single exponential decay of the IR-RF dose curves for all K-feldspars. Trautmann et al. (1999a,b) and Trautmann (2000) presented dating results, which mostly agreed very well with other dating results. Krbetschek et al. (2000) summarised methodological aspects of the IR-RF technique and Krbetschek and Trautmann (2000) investigated the dosimetric RF behaviour of other materials such as quartz and halite. Trautmann et al. (2000) presented a spectral study of single feldspar grains and pointed out the potential of IR-RF single grain dosimetry. The challenge of a very precise beta source calibration for the IR-RF technique has been solved by the indroduction of a radiofluorescence method using Al_2O_3:C crystals as probe dosimeters (Erfurt et al. 2000; Erfurt et al. 2001). Together with an automated multi-spectral radioluminescence (RL) reading system for geochronometry and dosimetry, Erfurt et al. (2002) precisely described the calibration protocol using the RF at 415 nm of Al_2O_3:C dosimeters. They also reported on dating results which correspond very well with independent ages. Furthermore, the physical background and the methodology of the IR-RF dating technique were investigated by Erfurt and Krbetschek (2002) and, among other things, they found, that the IR-RF dose curves can be modelled more precisely using a stretched single exponential decay. They also suggested the use of a combination of additive dose and regeneration dose curves (slide technique) for the estimation of the palaeodose. Schilles and Habermann (2000) and Schilles (2002) reported on an experimental device for the measurement of IR-RF of K-feldspar and physical features of this emission.

In this paper we present state-of-the-art knowledge of the methodology of the IR-RF dating technique, resulting in a standard single-aliquot regenerative-dose protocol, called IRSAR.

3. Measurement conditions

3.1 IR-RF instrument

All measurements were carried out using the automated multi-spectral radioluminesence (RL) instrument described by Erfurt et al. (2002).

3.2 Sample preparation and geological settings

All samples were prepared using standard procedures (Aitken 1998). Geological settings and detailed sample preparation descriptions of the samples (GOS4, HURL1, SHO, GRÖ8 and OOK1) can be found elsewhere (Preusser 1999; Erfurt et al. 2002; Trautmann et al. 1999b). From the IR-RF measurements already carried out, it was clear, that samples that were additionally treated by flotation to extract the whole feldspar fraction before the K-feldspars were separated by density, showed much higher IR-RF intensities. Therefore we used the flotation technique to extract quartz from feldspar as described by Miallier et al. (1983)

3.3 Physical and methodological requirements of IR-RF dosimetry for sediment dating

This new IR-RF dating technique is characterised by the following methodological features:

- Extracted K-feldspars which underwent flotation, prior to being separated by density, showed stronger IR-RF intensities; this may indicate enhanced enrichment of K-feldspars (Erfurt et al. 2002)
- Due to the continuous excitation by ionising radiation and the simultaneous observations fluorescence, the method is a single-aliquot technique with only one regenerative dose cycle compared to the commonly used SAR protocols applied to quartz and feldspar (Murray and Wintle 2000; Wallinga et al. 2000)
- The RF spectra of K-feldspars show, an interfering RF peak at about 710 nm; this has to be considered when filters for the isolation of the IR-RF peak are chosen (figure 3)
- The IR-RF dose curves follow a stretched single exponential dose curve function (Erfurt et al. 2002) with non-significant fit residual (see figures 4 and 5)
- After bleaching by light with solar emission characteristics, the samples exhibit strong phosphorescence (figure 6)
- Since the IR-RF is measured continuously during interaction with ionising radiation, all transitions of charges in the material are characterised by a dynamic (transient) equilibrium which compares to processes taking place in the radioactive environment of the sediments (Erfurt and Krbetschek 2002)
- Compared with secondarily excited radiophosphorescence techniques, such as TL and OSL, IR-RF the dosimetric informations based primarily on excited electronic transitions and the electron density in the IR-RF (IR-OSL) trap is monitored (Erfurt and Krbetschek 2002)
- The method does not need thermal pre-treatment of samples and the IR-RF shows no change in the dose curve response during regeneration cycles (figure 4)
- The mean saturation dose is about 1200 to 1500 Gy. However, due to the small dynamic range of the IR-RF process and the decrease of the sensitivity with dose, the dose curves are resolvable up to about 600 to 800 Gy (Erfurt et al. 2002)

- The IR-RF trap shows very high thermal stability. There is no significant change in the dating results if the samples are heated up temperatures ranging from 250 to 350°C (figure 7)

3.3.1 Spectral aspects, filter choice

Krbetschek et al. (2000) mentioned IR-RF detection problems that may result from the interference of a neighbouring RF emission band at 710 nm. For a better understanding of filter selection, we have used a Gaussian distribution function in order to simulate different interference ratios for the RF Gauss peaks, separated by different filters (resulting spectra in figure 3). To simulate the "worst case" scenario, we used the mean Gaussian fit data of saturated K-feldspars (about 1500 Gy) with a very strong emission at 710 nm.

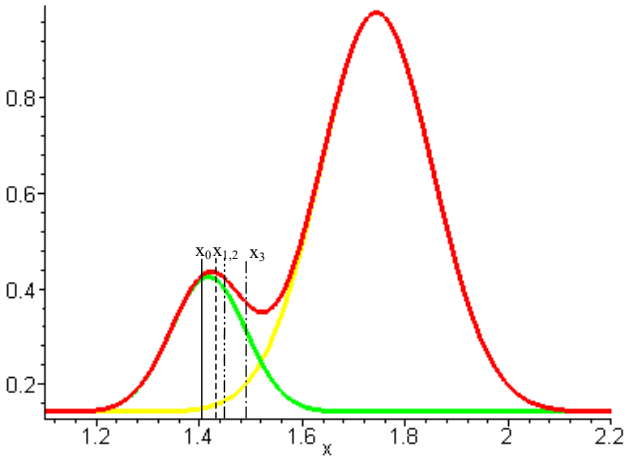

Figure 3.
Simulated saturated spectrum generated by mean values of Gaussian distributions from an number of RF spectra of K-feldspars in the energy range from 1.2..2.0 eV. The vertical lines indicate the integration intervals ($x_0..x_1$ = Andover 200FC35-25/8650, $x_0..x_2$ = Schott RG850, $x_0..x_3$ = Schott RG830)

An interference filter (Andover 200FC35-25/8650) with a bandwith of 18.7 nm FWHM (after Erfurt et al. (2002)) and the characteristics of the Schott RG850 and Schott RG830 filters (suggested as the detection window by Schilles (2002)) have been used as the integration regions. This Gaussian distribution of the spectrum was integrated (fig. 1) at 50 % transmission for all filters (see figure 3: $x_0..x_3$ as integration intervals for the simulation of different filter transmissions). The results of this simulation were corrected for the changing detector sensitivities in this wavelength interval. The computed percentage of the simulated signal overlapping are for the interference filter (Andover 200FC35-25/8650) 5.2%, for the Schott RG850 6.4% and for the Schott RG830 12.1%. Typical values for signal interference (e.g. sample Bur10, described by Krbetschek et al., 2000) were estimated using this spectral simulation. The ratios were not more than 0.9% for the Andover 200FC35-25/8650, 1.0% for the RG850 and 1.8% for the RG830. In contrast to Schilles (2002), we do not recommend using filters which transmit below 840 nm. Optimal results can be reached using an interference filter centred around the IR-RF emission at 865 nm, such as the previously mentioned Andover 200FC35-25/8650 or with much higher transmittance (but also much more expensive), filters of the Chroma Technology HQ series (HQ865/20M). However, since the IR-RF signals are the strongest RF emissions in microcline and orthoclase, the typically low transmission percentages of interference filters (of only about 40 to 50%) still leads to sufficient PMT counting statistics.
The emission at 920 nm in K-feldspar (Erfurt and Krbetschek 2002) does not have an influence on the dose characteristics of the the 865 nm peak; this is because of the very low sensitivity of the used Hamamatsu PMT R943-02 in this wavelength region (Erfurt et al. 2002).

3.3.2 Dose curve fitting

The experimental data and the luminescence model suggested by Trautmann (2000) give a single exponential dose curve function which described the IR-RF data. The IR-RF was measured using RF spectra together with a Gaussian distribution of the spectra. Only a maximum of about 30 dose points were used for the single exponential fit function. Using the automated RL instrument (Erfurt et al. 2002), commonly about 200 and up to 800 dose points are measured depending on the absorbed dose. Such a high data density results in a very precise dose curve record. It has been observed by Erfurt and Krbetschek (2002) that the IR-RF dose characteristic does not exactly follow a strict single exponential function. Therefore they suggested, that a stretched exponential function (equation 1) can describe a behaviour which is often encountered in disordered condensed-matter systems (e.g. by Pavesi and Ceschini (1993)).

$$(1) \qquad \Phi(D)=\Phi_0-\Delta\Phi(1-\exp(-\lambda D))^{\beta}$$

(Φ_0..initial IR-RF flux, $\Delta\Phi$..dose dependent change of the IR-RF flux, λ..exponential parameter, D..dose, β..dispersive factor)

They suggested that the dispersion of charge carrier transition or release rates and trap energies in

multiple trapping-detrapping mechanisms can be expressed in the dispersive factor β in equation 1. Erfurt and Krbetschek adapted such a function for the IR-RF dose curve description and discussed its influences on the model indroduced by Trautmann (2000).

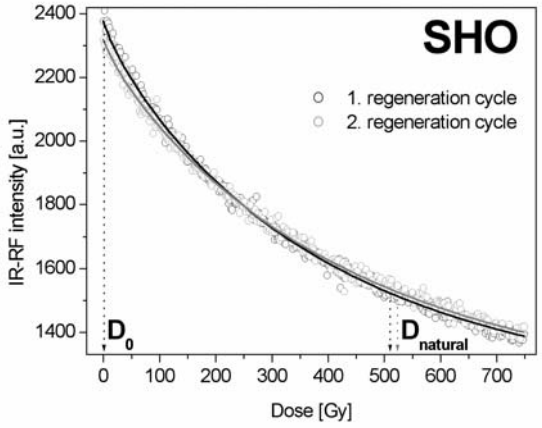

Figure 4.
Dose curves of regeneration cycles of sample SHO. One can see the very good fitting of a stretched exponential function to the IR-RF data. Also slight changes in the luminescence response after a second regeneration cycle resulting in only a very small change of the dose determination are visible.

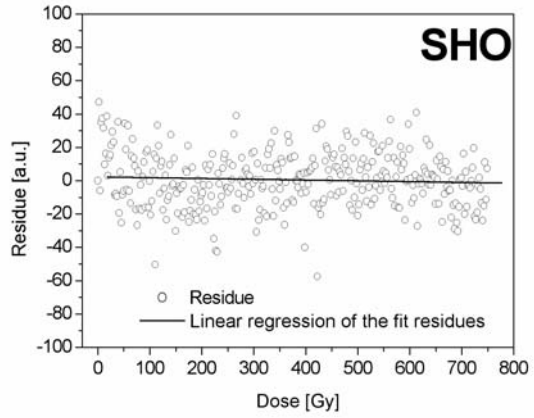

Figure 5.
Fit residual of the IR-RF dose curve fit of sample SHO (figure 4) using equation 1. The residual were fitted using a linear regression function. One can see the precision of the parameter determination using this stretched single exponential fit function. Together with the high number of measured dose points (a few hundreds) the IR-RF data show good agreement of experimental observation and theoretical considerations (Trautmann 2000, Erfurt and Krbetschek 2002).

Applying equation 1 to the data of figure 4, the dose curve of sample SHO can be described yielding residuals close to zero (figure 5) (more examples in Erfurt et al. (2002) and Erfurt and Krbetschek (2002)).

3.3.3 Effects after bleaching I: phosphorescence

Trautmann et al. (1999a,b) pointed out the spectral bleaching behaviour of the IR-RF signal and Krbetschek et al. (2000) discussed the implication for dating methodology. If the samples are bleached using the Osram HTI lamp (which is part of the RL instrument described by Erfurt et al. (2002)) K-feldspar show very strong phosphorescence at 865 nm. Figure 6 illustrates this effect, observed for a saturated sediment sample OOK1 (about 1500 Gy given dose). The decay of the phosphorescence is exponential. The phosphorescence was measured immediately after the bleaching light was shut off from the samples. Because of an 18 seconds time delay between shutter closing and the first phosphorescence measurement, we extrapolated the exponential decay function to the intitial phosphorescence as shown in figure 6.

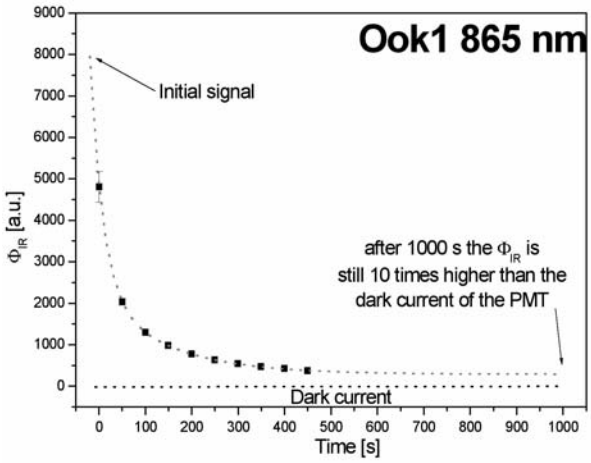

Figure 6.
Typical phosphorescence kinetics at 865 nm measured directly on sample OOK1 after bleaching for 30 minutes. The decay follows an exponential function and complete depletion of the signal is measured only after a few thousands seconds. This may interfere with the IR-RF signal, if regeneration is started immediately after bleaching.

The phosphorescence in figure 6 was measured for only 450 seconds. On extrapolation of the phosphorescence characteristics, one can see that the intensity is not completely decayed. Therefore, it is important to wait about one hour after bleaching, before the regeneration of the palaeodose can be

started, because of a possible superposition of the phosphorescence after bleaching and the radiofluorescence.

3.3.4 Effects after bleaching II: changes in the IR-RF dose curve response

After a second regenerative dosing, the reconstructed dose curves show no significant differences from that of the first cycle. Figure 4 presents a typical example of a sediment sample (SHO). A change in the dose curve response is commonly expressed in terms of sensitivity changes.

As one can see in figure 4, such effects may occur to a small extent but do not change the dose reconstruction (using the IRSAR protocol) adversely. If a palaeodose would be estimated using these two regenerated dose curves applying the IRSAR protocol (see section 4), a deviation of only 3 % occurs (D_{black}=508.9 Gy and D_{grey}=525.9 Gy).

3.3.5 Saturation dose, signal stability and upper dating limit

Trautmann et al. (1999b) concluded from spectral measurements, that the IR-RF saturation dose lies at about 800 Gy. Measuring the IR-RF with higher dose resolution (number of measured dose points) using the automated RL instrument (Erfurt et al. 2002), a saturation dose of about 1200..1500 Gy was estimated (see figure 4). On the other hand, the technical dating limit depends mainly on the dynamics ($d\Phi/dD$) of the IR-RF signals at high given doses. Based on state-of-the-art knowledge, it can be assessed that the IR-RF dose curves are resolvable up to 650 Gy (Erfurt et al. 2002) and this results in an (mean) upper dating limit of around 250 to 280 ka, assuming a sediment dose rate of about 2.5 mGy a^{-1}. Thus, the high saturation dose together with the thermal stability of the IR-RF signal has potential to increase the upper age limit of luminescence dating. Figure 7 shows the thermal stability of the IR-RF signal after pulse annealing of sample SHO to 100°C, 175°C, 250°C and 350°C. The equivalent dose of sample SHO at room temperature is ≈ 600 Gy. The reconstructed dose after a preheat only slightly changes, giving values at 100°C ≈ 595 Gy, 175°C ≈ 580 Gy and 250°C ≈ 565 Gy. After annealing up to 350°C, the signal is altered and the reconstructed dose equals to ≈ 515 Gy. This test implies, that the IR-RF signal seems to be thermally stable up to about 250°C.

4. The dating protocol IRSAR (infrared radiofluorescence single-aliquot regeneration)

Summarising all aforementioned methodological aspects, we describe in the following the IRSAR (infrared radiofluorescence single-aliquot regeneration) dating protocol.

The IRSAR protocol applied to the IR-RF on K-feldspar:

1. Separation of K-feldspars using standard procedures combined with the flotation technique to separate quartz from feldspars
2. Measuring of the IR-RF intensity at natural dose D_N
3. Bleaching of samples under solar conditions for 30 minutes without changing the geometry
4. Waiting for at least one hour until the phosphorescence excited by the bleaching light is decays completely
5. Regeneration of the IR-RF signal to the natural dose level with preferably a high number of dose points
6. Fitting data to a stretched single exponential function (equation 1)
7. Using fit parameters (Φ_0, $\Delta\Phi$, λ and β) and the IR-RF signal ($\Phi(D)$) at the natural dose level to calculate the palaeodose D

After an investigation by Erfurt et al. (2002), the application of the protocol is also shown in figure 8. The first step is the measurement of $\Phi_{natural}$ connected to the palaeodose D_e.

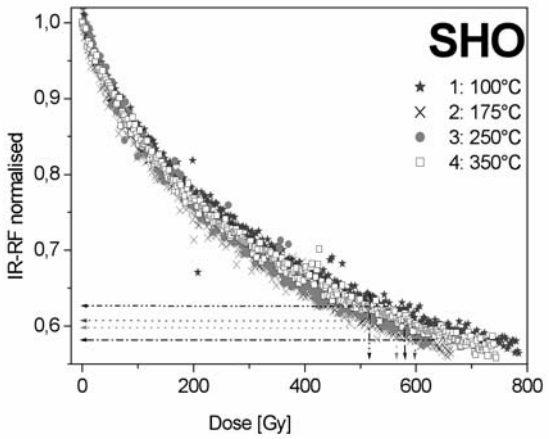

Figure 7.
Comparison of IR-RF dose curves after preheat of 100°C (grey stars), 175°C (black crosses), 250°C (grey circles) and 350°C (open black squares). Comparing the determined equivalent dose for the unheated sample of 598 Gy, the reconstructed doses of the preheated samples at 100°C (595 Gy), 175°C (580 Gy) and 250°C (565 Gy) only changes slightly. This indicates the high thermal stability of the IR-RF process.

During bleaching for 30 minutes, the IR-RF increases up to the maxiumum IR-RF signal $\Phi_{bleached}$. After bleaching the IR-RF signal $\Phi_{natural}$ related to the palaeodose D_e is regenerated, by measuring 200 dose points. The applied laboratory dose then equals the equivalent dose, absorbed during burial after the last light exposure of the sediment.

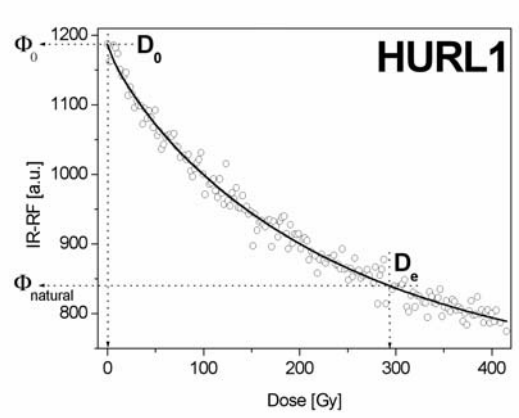

Figure 8.
IR-RF dating example applying the IRSAR protocol to sample HURL1 (Erfurt et al. 2002). The dose curve was measured by reading 200 dose points.

We propose to make a standard sample preparation, together with additional flotation before feldspar separation by density to enrich K-feldspars in the sample. Furthermore one should guarantee to have a packed mono layer of sample grains for dosimetric reasons. Therefore we suggest to use sample plates as described by Erfurt et al. (2002).
The palaeodose can also be estimated graphically. However it is more precise to calculate the palaeodose using equation 1.

A comparison of ages determined by the IRSAR protocol and ages estimated using IR-OSL, U/Th and ^{14}C is presented in figure 9 for sample GOS4, GRÖ8 and HURL1. This again underlines the good agreement of IRSAR data to other dating techniques.

8. Discussion and summary

We have presented a single-aliquot regenerative-dose protocol applied to the infrared radiofluorescence (IRSAR) of coarse-grain K-feldspar. It is a robust and precise method to determine the equivalent dose connected to the last light exposure of clastic Quaternary sediments with the possibility to observe the primary dating information in terms of the electron density in the IR-RF (IR-OSL) trap. The physical and methodological charcteristics show that this new promising technique does not need special treatment of the samples (e.g. for sensitivity changes), compared to other luminescence methods (SAR on quartz and feldspar). Furthermore, the IR-RF can be measured using a very simple experimental set-up. Based on state-of-the-art knowledge of the physical background, we assume a reliable dating range from about 10 ka over up to over 250 ka. With regard to the saturation dose levels as well as the thermal stability of the IR-RF signal, there is some potential to increase the upper dating limit.

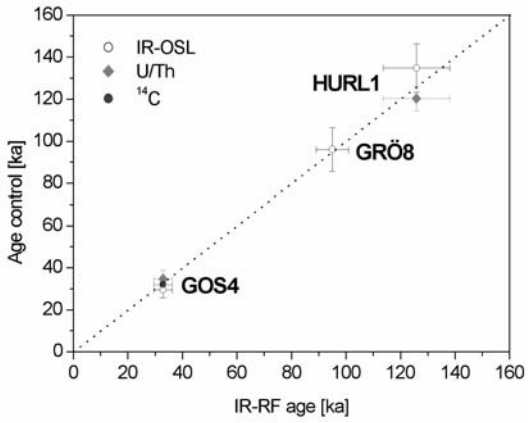

Figure 9.
Comparison of IR-RF ages with IR-OSL, ^{14}C and U/Th ages (data after Trautmann et al. (1999) and Erfurt et al. (2002)) of samples GOS4, GRÖ8 and HURL1

However, much more work is needed to investigate the IR-RF more precisely, especially its behaviour at higher dose levels as well as on effects which may affect the stability of the transient equilibrium of the fluorescence occurring during interaction of the minerals with ionising radiation.
This paper should encourage the luminescence dating community to apply and to investigate this new IR-RF dating technique.

Acknowledgements
We gratefully thank Dr. F Preusser (Köln and Bern Universities) for providing material of samples GOS4 and HURL1. This research work is financed by the German Ministry of Education and Research (BMBF) under contract 03KR9FR2/7.

Purchase of IR-RF instrumentation
If there are questions about the purchase of IR-RF instrumentation, please ask the corresponding author.

References

Aitken M. J. (1998) *An indroduction to optical dating.* Oxford University Press. Oxford, U.K.

Erfurt G.; Krbetschek M. R.; Trautmann T. and Stolz W. (2000). Radioluminescence (RL) behaviour of Al_2O_3:C - potential for dosimetric applications. *Radiat. Meas.* **32**, 735-739

Erfurt G.; Krbetschek M. R.; Trautmann T. and Stolz W. (2001). Radioluminescence (RL) probe dosimetry using Al_2O_3:C for precise calibration of beta sources applied to luminescence dating. *Radiat. Phys. Chem.* **61**, 721-722

Erfurt G.; Krbetschek M. R.; Bortolot V. J. and Preusser F. (2003). A fully automated multi-spectral radioluminescence reading system for geochronometry and dosimetry. *Nucl. Instr. Meth. Phys. Res. B*.207 (4), 487-499.

Erfurt G. and Krbetschek M. R. (2003). Studies on the physics of the infrared radioluminescence of potassium feldspar and on the methodology of its application to sediment dating. *Radiat. Meas.*, Vol.**37**, 505-510.

Krbetschek M. R.; Trautmann T.; Dietrich A. and Stolz W. (2000). Radioluminescence dating of sediments: methodological aspects. *Radiat. Meas.* **32**, 493-498

Krbetschek M. R. and Trautmann T. (2000). A spectral radioluminescence study for dating and dosimetry. *Radiat. Meas.* **32**, 853-857

Miallier D.; Sanzelle S. and Fain, J. (1983). The use of flotation technique to separate quartz from feldspar. *Ancient TL* **1**, 5-6

Murray A. S. and Wintle A. G. (2000). Luminescence dating of quartz using an improved single-aliquot regenerative-dose protocol. *Radiat. Meas.* **32**, 57-73

Preusser F. (1999). Luminescence dating of fluvial sediments and overbank deposits from Gossau, Switzerland: fine grain dating. *Quat. Geochr.* **18**, 217-222

Rutherford E. (1911). The scattering of α and β particles by matter and the structure of the atom. *Phil. Mag.* **21**, 669-688

Schilles T. und Habermann J. (2000). Radioluminescence dating: the IR emission of feldspar. *Radiat. Meas.* **32**, 679-688

Schilles (2002). Die Infrarot-Radiolumineszenz von Feldspäten und ihre Anwendung in der Lumineszenzdatierung. *PhD thesis*. Ruprecht-Karls-Universität Heidelberg

Trautmann T.; Krbetschek M. R.; Dietrich A. and Stolz W. (1998) Investigations on radioluminescence of feldspar: Potential for a new dating technique.- *Radiat. Meas.* **29**, 421

Trautmann T.; Krbetschek M. R.; Dietrich A. and Stolz W. (1999a). Radioluminescence Dating: A New Tool for Quaternary Geology and Archaeology. *Naturwissenschaften* **86**, 441-444

Trautmann T.; Krbetschek M. R.; Dietrich A. and Stolz W. (1999b). Feldspar radioluminescence: a new dating method and its physical background. *J. Lum.* **85**, 45-58

Trautmann T.; Krbetschek M. R.; Dietrich A. and Stolz W. (2000). A systematic study of radioluminescence properties of single feldspar grains. *Radiat. Meas.* **32**, 685-690

Trautmann T. (2000). A study of radioluminescence kinetics of natural feldspar dosimeters: experiments and simulations. *J. Phys. D: Appl. Phys.* **3**, 2304-2310

Wallinga, J., Murray A. and Wintle A. (2000). The single-aliquot regenerative-dose (SAR) protocol applied to coarse-grain feldspar. *Radiat. Meas.* **32**, 529-533

Rewiever

Ann Wintle

Source calibrations and blind test results from the new Luminescence Dating Laboratory at the Instituto Tecnológico e Nuclear, Sacavém, Portugal

D. Richter*, A.J.C. Zink, K.R. Przegietka, G.O. Cardoso, M.A. Gouveia & M.I. Prudêncio
Instituto Tecnológico e Nuclear, Estr. Nac. 10, 2686-953 Sacavém, Portugal
* Corresponding author: richter.hdh@freenet.de

(Received 10 April 2003; in final form 30 May 2003)

abstract : *Blind test results for the most important materials used in luminescence dating are reported as a measure of the quality of performance of the new luminescence dating laboratory at the Instituto Tecnológico e Nuclear, Sacavém, Portugal. At the same time they serve as a measure of the quality of the source calibrations, which are outlined as well, and an estimation of the required charge particle equilibrium (CPE) distance for gamma irradiation of the calibration material is presented. Several different quartz and measurement techniques are employed for the calibration of alpha and beta sources.*

Introduction

The desire of the Portuguese archaeology for chronometric dating tools in addition to the existing radiocarbon facility led to a protocol between the Instituto Português Arqueologia (IPA) and the Instituto Tecnológico e Nuclear (ITN), in order to set up a luminescence dating facility at the latter. Building work was finished in spring 2001, and the laboratory completed in fall 2002. The task was to set up a basic luminescence dating laboratory, which is able to perform dating application on the following most common minerals/materials used in luminescence dating for archaeology and geology:

- polymineral fine grain sediment (feldspar)
- coarse grained sediment (quartz)
- archaeological heated material (ceramic, pottery, brick, tile, etc.)
- SiO_2-bearing heated archaeological material (silex, chert, etc.)

Additional, but less frequently used, techniques like fine grain quartz or coarse grain feldspar sediment dating can be implemented easily in the future. The primarily function of the laboratory is supposed to be of service.
In order to test the laboratory's performance, a quality insurance program was started by measuring samples, which have already been dated by established luminescence dating laboratories. At the same time, these tests are a check of the calibration of the radioactive sources used at ITN.

The new laboratory

The new laboratory consists of three connected rooms (sample preparation, measurement and irradiation). R10 Encapsulite fluorescent tubes provide the lighting in all rooms. The laboratory is equipped with all the standard chemicals and equipment for the physical and chemical sample preparation employed in luminescence dating. The luminescence reader is a Risø DA-15 with an additional halogen lamp. Two systems were set up for measuring the external gamma dose rates. A portable γ-spectrometer (Target NanoSpec) was calibrated versus the Oxford and the Gif-sur-Yvette blocks, and a system based on α-Al_2O_3:C (TLD-500) dosimeters was developed (Richter & Zink). Furthermore, Neutron Activation Analysis (NAA) is an already well-established tool at ITN (Gouveia et al., 1992).
Grants for upgrading this basic laboratory with equipment like a single-grain luminescence reader and a low level γ-spectrometer are pending.

Beta-source calibration and estimation of Charged Particle Equilibrium (CPE) condition

Two $^{90}Sr/^{90}Y$-beta-sources are employed at the laboratory. One (nominal 40 mCi) is attached to the luminescence reader and the other one is a stand-alone 30-positions irradiator by Daybreak (801E, nominal 200 mCi).

A total of three different quartz samples and three different protocols with TL and B-OSL were used for calibration of these beta-sources.

The Risø calibration quartz, as provided during installation of the system, is sedimentary quartz from Jutland, which was annealed at 500ºC and irradiated with a ^{137}Cs source. After corrections for attenuation

the absorbed dose to the quartz is given as 4.45 ± 0.07 Gy (A.Murray, information sheet for calibration quartz). A B-OSL SAR protocol (Murray and Wintle, 2000) with 3 dose points was used for estimating the dose rates of the ITN beta sources.

The GSF quartz was kindly provided by H.Y. Göksu, and is from the same batch as described in Göksu et al., 1995, but of a different irradiation with a ^{60}Co source. The absorbed dose is given as 0.5 ± 0.015 Gy. Measurements followed as outlined in Göksu et al., 1995. A wide integration range was employed for the blue TL (7-59 and HA-30). A beta dose comparable to the gamma dose was given to aliquots with material identical to the quartz prior to gamma irradiation. All data were normalized by a second glow, and the ratio of integrated beta and gamma irradiated luminescence gave the calibration value. Some B-OSL measurements (see Risø calibration quartz) were performed as well.

In order to ensure the laboratories independence, commercial Merck quartz (107536 quartz, washed and calcined, charge TA 1077836 204, 0.2 - 0.8 mm) was purchased, prepared and irradiated with a ^{60}Co source at ITN (Oliveira, et al., 2000). Some of this quartz was further crushed with an agate mill prior irradiation. Tests revealed that the sensitivity could be increased and sensitivity changes decreased by a repetition of rapid heating to 700ºC and fast cooling, followed by HCl-washing after the last cycle. Long heating was found to decrease the sensitivity and a further sensitization by beta irradiation in between heating cycles to be unnecessary. The gamma irradiation was performed on a dense mix of grain sizes between 0.001 mm and about 1.0 mm, in order to allow the irradiation of a dense material with the least cavities. It is thus assumed that any corrections for interactions at repeated air-grain boundaries are not necessary. The required container thickness to obtain charged particle equilibrium (CPE) for ^{60}Co-irradiation was estimated for fused (pyrex) quartz of 2.23 g cm^{-3} density, using mass stopping power values provided by the ESTAR (NIST) database (ESTAR). It is assumed that CPE is reached in matter at a distance equivalent to the maximum electron pathlength. As we were unable to find sufficient data for secondary electrons, the upper limit estimate of the range of penetration was calculated assuming electron energy to be equal to the total photon energy, which is certainly a slight overestimation. Additionally, the average range of penetration is smaller than the average pathlength because the trajectory of electrons in solids is zigzak-like. We further assume, that for energetic photons (above 200 keV) the photoelectric electrons originate mainly as result of interaction of secondary (Compton) photons with the mater, and any effect of Bremsstrahlung is negligible. The obtained value of 3.6 mm as the required thickness to reach CPE is in good agreement with empirical data, indicating 3 mm to 4 mm (pers. comm.. H.Y.Göksu).

Employing the mass absorption coefficients of the XAAMDI (NIST) database and from Aitken, 1985, we obtain for ^{60}Co a ratio of 0.996 (0.0266/.0267, the latter interpolated for 1.17 and 1.33 MeV), in order to convert for Air Kerma to gray (Gy) in quartz.
The self-attenuation of a sample can be calculated in a simplified approach by the following formula:

$$D = D_O * (1 - mu*r/3), \quad (1)$$

where D is the attenuated dose of gamma radiation, D_O is the dose delivered by the source, mu is the linear attenuation coefficient of the sample, r is the inner radius of the container (or half of the length of the base in the case of quadratic base containers)

This formula (1) was derived for homogenous and isotropic radiation around a container of overall small dimensions, as compared to the mean free path of gamma photons (mu*r << 1). For ^{60}Co irradiation we found the self-attenuation factor to be 0.985.

Specially build fused quartz containers of quadratic base with 3.6 mm wall thickness and 8.0 mm inner base-length were employed for ^{60}Co (nominal 300 Ci) irradiation equivalent from all four sides. Any attenuation due to the thickness of the "sample" for such irradiation is assumed to be similar as resulting from homogenous and isotropic radiation field. Applying the above, the total absorbed dose in our case is 1.96 ± 0.018 Gy.
After irradiation the 90-160 μm fraction was obtained by dry-sieving and the 4-11 μm fraction was extracted by settlement in acetone. TL measurements were performed using a blue detection window (7-59 + HA-30). The peak-integrated TL from the gamma irradiated material was matched to the linear regression of 3 dose points from beta irradiated material. Additionally, a portion of the zeroed material was given a ^{137}Cs dose of 2.0 Gy at the Gif Luminescence Laboratory (LSCE at the CNRS-CEA), and measured in the same way.

Some measurements were performed with and without silicon oil as a fixing agent. Only an insignificant tendency to slightly lower results with silicon was observed. All the results are corrected for a common date of 12/10/2002 (Table 1).

	Risø-β		Daybreak-β	
	B-OSL	TL	B-OSL	TL
GSF	5.68*; 5.56	5.78	n.a.	12.69#
Risø	5.69*; 5.55	n.a.	Failed	n.a.
ITN-Merck	n.a.	5.54	n.a.	12.82
CNRS-Merck	n.a.	n.a.	n.a.	12.49
ITN-Merck fine	n.a.	4.52	n.a.	10.18

Table 1.
*Summary table of calibration results. All values in Gy min^{-1}, corrected for a common date of 12/10/2002. For clarity the error estimates are omitted. * not fixed with silicone oil. # average of 4 measurements with 10 gamma and 10 beta irradiated cups.*

Alpha source calibration

The Littlemore 6-seater alpha irradiator (type 721A, AMM3, nominal 182 mCi) with ^{241}Am-foils was calibrated by the manufacturer with a low level alpha counter under vacuum. This calibration was verified by the blind tests and additional measurements of a polymineral fine-grained sample (HDS-243; loess), which exhibits a linear alpha-dose growth and no fading (kindly provided by the the Forschungsstelle Archäometrie am MPI für Kernphysik, Heidelberg). Natural material (4-11 μm) was irradiated at Heidelberg with an identical alpha irradiator of a different activity, which was calibrated in 1978 by the manufacturer. Some of the natural material was irradiated (on disc) with five different alpha doses at ITN, with dose points set to be lower, about equal and higher than the Heidelberg irradiation, while other discs were left unirradiated (natural). The IRSL was measured after storage at 70ºC for one week, following the Heidelberg protocol as closely as possible. The Heidelberg irradiated material could not be normalized by a short shine because it had to be scraped off the discs after irradiation and re-deposited at ITN. Therefore a normalization by a beta dose after the first readout was employed. Subsequently a D_E-alpha was calculated using only the natural and ITN irradiated material and compared to the result obtained in Heidelberg (Table 2). The result of the measurement of the Heidelberg irradiated material was then plotted against values obtained for ITN irradiated discs. This gave the dose rate of the ITN source relative to the Heidelberg source by matching the luminescence of the former versus the linear fit of the latter (Table 2).

Littlemore calibration (μm^{-2} min^{-1}) *	0.191
Calibration versus Heidelberg (μm^{-2} min^{-1})º #	0.215
D_E-α Heidelberg (μm^{-2})º	67.88 ± 7.48
D_E-α ITN (μm^{-2}) #	79.55 ± 8.1

Table 2.
*Results obtained for fine grain material of sample HDS-243, as verification of alpha source calibration. * average of five out of six positions, as one position is significantly different then the others and is thus not used. º corrected for decay since calibration. # Based on the integrated luminescence of the first 20 s (last 10 s background subtraction) of 60 s room temperature stimulation by IRSL at 35% to adjust for the higher power of the DA-15 versus DA-12 system (30 % roughly equals, pers. comm. S. Lindauer), using a blue detection window (set of BG39, BG3, GG400, BG3), after a preheat of 220ºC for 2 min.*

The results cannot be regarded as independent, as, presumably, the manufacturer used the same method for calibrating both sources. Nevertheless, giving the long time span between these calibrations, the parameters (equipment, etc.) were certainly not identical. The result of the calibration versus the Heidelberg source of 0.215 μm^{-2}min^{-1} shows good agreement with the manufacturers average value of 0.191 μm^{-2}min^{-1}, as do the D_E-α determinations of 67.88 ± 7.48 μm^{-2} at Heidelberg and 79.55 ± 8.1 μm^{-2} at ITN, which both employ the calibration values given by the manufacturer. This gives confidence in the determination of the alpha sensitivity at ITN.

The blind test samples

The purpose of the exercise was to test the quality of luminescence dating at the new laboratory at ITN, with the protocols established there. Therefore only the palaeodoses and the alpha sensitivities (where applicable) are reported here. The dosimetric tools for determining the dose-rates are either already evaluated (Gouveia et al., 1992) or will be presented separate by Richter & Zink, 2003.

The luminescence parameters for the following four different samples, representing the most important materials used in luminescence dating, were determined:

- loess from Nussloch (Germany), provided by the Geography Department, University Bonn
- heated flint from the Upper Palaeolithic site Geißenklösterle (Germany), provided by the Forschungsstelle Archäometrie, Heidelberg

- dune quartz from the Southern United Arab Emirates, provided by the School of Geography and the Environment, Oxford
- brick from St. Denis (France), provided by the C2RMF Louvre, Paris

Unprepared portions were received for all four samples and the full preparation cycle was performed at ITN. With the exception of the heated flint, the tests were true blind tests.

The fine grain sediment sample is loess originating from the long sequence at Nussloch in Germany. It is used in an intercomparison of German luminescence dating laboratories (Mauz et al., 2003), and soon will become an internationally recognized standard for γ-spectrometry. Results from two participating laboratories are published by Mauz et al., 2003, who also summarize the standard sample preparation procedures. Five different methods were used in order to establish the parameters of equivalent dose and alpha sensitivity. Additive dose TL and IRSL-methods were applied, as well as SAR-IRSL and post IR B-OSL-SAR.

The heated flint was previously measured at the Forschungsstelle Archäometrie am MPI für Kernphysik, Heidelberg. The results are published as sample GK8 in Richter et al. 2000, thus this sample cannot be regarded as a true blind test. Sample preparation followed as outline by Aitken, 1985 and Richter et al., 2000. The palaeodose was determined by the additive dose and regeneration methods, and the additive method for the alpha sensitivity.

The School of Geography and the Environment, Oxford provided a coarse grain quartz sample. It originates from 22 m depth of a core (LIWA2) of a dune in the Southern United Arab Emirates. The Oxford laboratory employed a B-OSL SAR protocol on the coarse grain quartz fraction, using preheats of 260ºC for 10s for 0, 3, 6, 3, 0 Gy regeneration doses, with a 1 Gy test dose for 190 aliquots. An almost identical protocol was employed at ITN as well, with a variation of the regeneration doses.

The brick sample was provided by the Centre de Recherche et Restauration des Musées de France, Louvre, Paris (C2RMF). The preparation of the polymineral fine grain sample was performed according to Aitken 1985. All measurements reported here are TL, using the additive and the regeneration methods. The alpha sensitivity was determined by the additive dose technique.

Blind test results

The results (Table 3) are reported, grouped by sample and technique, together with the values obtained by the other laboratories. The true ages of all samples are unknown. Therefore, only the difference between the determined results on the identical (or almost identical) samples versus the average of all results can be employed as a measure of the quality of the ITN laboratory performance (Table 5). This is applicable despite the fact, that the number of determinations exceed two in only one case.

The values in Table 5 show no systematic difference, neither towards over- nor under-estimation. The mean deviation from the average for the palaeodose determination is 3.64 % and 20.71 % for the a-value determination. The large value for the latter is not surprising, as it combines the differences in alpha and beta source calibration and their associated errors between the laboratories.

Discussion

The differences in calibration values obtained for all samples used are small, and agree very well to each other. As the grain sizes are similar, the average values are employed for each source in routine dating at ITN. It is anticipated to perform more measurements on other fine grain material in order to strengthen the calibration of the $^{90}Sr/^{90}Y$-beta-sources at ITN.

The discussion of the blind tests will be limited to the comparison of only the methods where results from other laboratories are available, and separated for the two parameters determined (where applicable the palaeodose is $D_E + D_I$) (Table 4).

Conclusions

The values obtained for beta source calibrations from the different materials and techniques exhibit a small spread, which allows the calculation of an average value as estimate of the source dose-rates. It also indicates the validity of all gamma irradiations with regards to the irradiation setup and calculation of the absorbed dose (e.g. estimation of distance needed for CPE).

The calibrations of the alpha sources are in good agreement, and the calibration by the manufacturer is preferred, as it is of primary significance.

The overall agreement of the blind test results from the ITN luminescence dating laboratory with the values obtained independently by other laboratories is fully satisfactory. Indirectly it indicates the validity of the source calibrations as well. It was shown that the new luminescence dating laboratory at ITN can provide satisfactory dating results for the four most important materials (fine grain polymineral sediment, quartz from sediment, ceramics and flint) employed in luminescence dating.

SAMPLE	METHOD	PARAMETER	OTHER LAB1	OTHER LAB2	ITN LAB
Loess	TL additive	D_E (Gy)	-	-	63.7 ± 5.7
	TL additive	a-value	-	-	0.024 ± 0.01
	IRSL additive	D_E (Gy)	59.8 ± 14.6	62.4 ± 5.4	57.1 ± 1.6
	IRSL additive	a-value	-	0.09 ± 0.01	0.05 ± 0.01
	SAR-IRSL	D_E (Gy)	-	-	56.9 ± 7.4
	SAR-post IR (B-OSL)	D_E (Gy)	-	-	61.8 ± 6.8
Silex	TL additive	D_E (Gy)	-	8.17 ± 0.06	8.37 ± 0.35
	TL regeneration	D_I (Gy)	-	2.87 ± 0.40	2.86 ± 0.30
	TL additive	a-value	-	0.23 ± 0.03	0.15
Quartz	B-OSL	D_E (Gy)	-	4.64 ± 0.45	4.01 ± 0.20
Brick	TL additive	D_E (Gy)	-	2.6 ± 0.3	2.7 ± 0.08
	TL regeneration	D_I (Gy)	-	-0.8 ± 0.6	0.0 ± 0.08
	TL additive	a-value	-	0.09	0.07

Table 3. *Results of luminescence measurements at ITN and other laboratories of the four blind test samples. D_E is the β-equivalent dose and D_I is the supralinearity correction.*

SAMPLE	PARAMETER	OTHER LAB1	OTHER LAB2	ITN LAB
Loess	D_E (Gy)	59.8 ± 14.6	62.4 ± 5.4	57.1 ± 1.6
	a-value	-	0.09 ± 0.01	0.05 ± 0.01
Silex	Palaeodose (Gy)	-	11.04 ± 0.46	11.23 ± 0.46
	a-value	-	0.23 ± 0.03	0.15 ± 0.05
Quartz	D_E (Gy)	-	4.64 ± 0.45	4.01 ± 0.20
Brick	Palaeodose (Gy)	-	2.6 ± 0.3	2.7 ± 0.08
	a-value	-	0.09 ± 0.01	0.07 ± 0.01

Table 4. *Luminescence results obtained at ITN versus results of other laboratories.*

SAMPLE	PARAMETER	AVERAGE	ITN DEVIATION	ITN DEVIATION (%)
loess	Palaeodose (Gy)	59.77 ± 2.65	-2.67	4.47
	a-value	0.07 ± 0.03	-0.02	28.57
Silex	Palaeodose (Gy)	11.14 ± 0.13	0.09	0.81
	a-value	0.19 ± 0.06	-0.04	21.05
Quartz	Palaeodose (Gy)	4.33 ± 0.45	-0.32	7.39
Brick	Palaeodose (Gy)	2.65 ± 0.07	0.05	1.89
	a-value	0.08 ± 0.01	0.01	12.5

Table 5
Average results for the blind test samples. The deviation of ITN determination from these averages expressed in absolute and relative values.

Acknowledgements
We owe a very special thank to S.Lindauer, BSc.(Forschungsstelle Archäometrie, Heidelberg), for helping in questions of sample preparation, and especially for providing sample material and assistance in the α-source calibration. We would like to thank all the laboratories and persons who provided the blind test samples and made their data available, namely Dr. H.Bray (Oxford Luminescence Research Group),Dr. J.R.Gaborit (Louvre Museum, Paris), Dr. J.Castaing (C2RMF, Louvre), Dr. B.Mauz (University Bonn). Additionally we would like to thank Dr. A.Ferro de Carvalho (LMRIR at ITN), and Dr. N.Mercier (LSCE at the CNRS-CEA) who performed the gamma irradiations.

References
Aitken, M.J. (1985) Thermoluminescence dating. Academic Press, London.

ESTAR at http://physics.nist.gov/PhysRefData/Star/

Göksu, H.Y., Bailiff, I.K., Bøtter-Jensen, L., Brodski, L., Hütt, G. & Stoneham, D. (1995) Interlaboratory beta source calibration using TL and OSL on natural quartz. *Radiation Measurements* **24**, 479-483.

Gouveia, M.A., Prudêncio, M.I., Morgado, I. & Cabral, J.M.P. (1992) New data on the GSJ reference rocks JB-1a by instrumental neutron activation analysis. *Journal of Radioanalytical and Nuclear Cemistry, Articles* **158**, 115-120.

Mauz, B., Bode, T., Mainz, E., Blanchard, H., Hilger, W., Dikau, R. and Zöller, L. (2002). The luminescence dating laboratory at the University of Bonn: Equipment and procedures. Ancient TL, **20**, 53-61.

Murray, A.S. & Wintle, A.G. (2000) Luminescence dating of quartz using an improved single-aliquot regenerative-dose protocol. *Radiation Measurements* **32**, 57-73.

Oliveira, C., Salgado, J., Ferro de Carvalho, A. (2000) Dose rate determinations in the Portuguese Gamma Irradiation Facility: Monte Carlo simulations and measurements. *Radiation Physics and Chemistry* **58**, 279-285.

Richter, D., Waiblinger, J., Rink, W.J. & Wagner, G.A. (2000) Thermoluminescence, Electron Spin Resonance and 14C-Dating of the Late Middle and Early Upper Palaeolithic Site Geißenklösterle Cave in Southern Germany. *Journal of Archaeological Science* **27**, 71-89.

Richter, D. & Zink, A. (2003) A small intrusion γ-dose rate measurement system based on the optical zeroing and read out of α-Al_2O_3:C (TLD-500) dosimeters. (to be submitted to Ancient TL).

XAAMDI at http://physics.nist.gov/PhysRefData/XrayMassCoef/cover.html

Reviewer
G. Wagner

Thesis Abstracts

Thesis title : An investigation into the physics of the infrared excited luminescence of irradiated feldspars

Author : Michael Anthony Short
Grade : Ph.D.
Date : January 2003
Supervisor : D. Huntley
University : Simon Fraser

Infrared excitation of irradiated feldspars produces a luminescence glow in one or more broad emission bands. The processes are poorly understood, but they are suspected to occur in lattice defects, although their general identity is unknown. This thesis is about trying to understand more about the physics of these processes. I found the emission intensity increased as the temperature was increased above 20 C for emission bands with peak intensities at wavelengths around330, 400 and 570 nm, but the rate of increase dropped off for some samples as the temperature was increased over 80 C. These results were interpreted as being due to the excitation of different vibrational modes of the feldspar structure. The rate of decay in the emission intensity of one sample was independent of temperature. The latter was clear evidence against a model where charge is excited from a trap by a combination of both optical and thermal excitation. The emission intensities of some emission bands were dependent on the polarization of the infrared exciting light, and the emission itself was polarized in some cases. These results were explained by dipolar transitions occurring within unknown defect centres located at either the T1, M or OD lattice sites. This explanation was supported by studies on transitions within Fe+3 ions occupying known lattice sites. I also found that there was a small photoconductivity with green light excitation, but no measurable effect with infrared excitation. However I could not rule out the possibility that charge was excited to delocalised bands in both cases. A model is proposed to explain these results with one basic type of electron trap which is excited by the infrared light. The excited electron can either tunnel through to a recombination centre or it can be thermally excited to the conduction band or to a state just below the conduction band. Anion defects are shown to be possible centres for the traps. Changes in the fraction of electrons that tunnel to the recombination centres, and electron spin interactions are proposed as additional mechanisms that may also have some effect on the changes in emission intensity with temperature.

Thesis title: Spectral investigations of luminescence in feldspars

Author : Marc René Baril
Grade : Ph.D.
Date : December 2002
Supervisor : D. Huntley
University : Simon Fraser

Optical dating is a tool for dating the last exposure of minerals to sunlight. The technique relies on the optically stimulated luminescence of irradiated minerals, particularly quartz and feldspar. Despite the widespread use of feldspar in dating, very little is known about the defects that give rise to the luminescence in this mineral.

A new high-sensitivity spectrometer was constructed for measurement of the emission spectra of the infra-red stimulated luminescence (IRSL) for a wide range of feldspars, and an attempt made to correlate specific spectral features with feldspar type or elemental content. Comparison of the IRSL spectra with spectra of phosphorescence following - irradiation and the spectra of phosphorescence after illumination indicates that the emission spectra are highly dependent on the type of excitation. This is a clear indication that certain traps are connected to particular luminescence centers. This conflicts with the standard model involving recombination via the conduction band. Excitation spectra were also measured and these indicated that the IRSL excitation resonance near 1.45 eV sometimes exhibits a strong Lorentzian character. The excitation spectrum was generally similar for both the violet (3.1 eV) and yellow-green (2.2 eV) emission bands, was unaffected by the polarization of the excitation light, and was best described by a Voigt profile near the 1.45 eV resonance.

The luminescence decay with time was found to follow Becquerel's equation, I(t)=I0/(1+t/t0). In terms of the time-integrated applied excitation energy E, this decay law may be expressed as, I(E)=I0/(1+E/E0). The parameters E0 and were found to vary strongly with excitation photon energy. was found to increase with applied dose, but both and E0 were relatively unaffected by sample temperature.

Measurement of the initial rate of decrease of intensity with time, S0=-dI/dt, versus initial intensity I0, for a wide range of excitation photon energies from 1.2 eV to 2.54 eV indicated that the scaling S0 I02 holds for excitation photon energies from the infrared excitation resonance well into the visible band. This provides strong evidence that a single trap is involved in the luminescence.

Some emission and excitation spectra for inclusions in quartz are suggestive of these being feldspars.

Thesis title: Testing and application of luminescence techniques using sediment from the southeast African coast

Author: Simon Armitage
Defence date: February 2003
Supervisors: G. Duller and A. Wintle
Examiners: A. Murray and R. Lucas
University: University of Wales, Aberystwyth

This thesis aims to test the single-aliquot regenerative-dose (SAR) technique using a selection of sedimentary quartzes from the southeast African coast. In particular, the ability of the SAR technique to correct for changes in the sensitivity of the optically stimulated luminescence (OSL) signal, which occur during measurement sequences, was tested. In addition, the SAR technique was used to date samples from the Mozambican islands of Inhaca and Bazaruto.

Several components have previously been identified within the quartz OSL signal. A new slow-bleaching, thermally-unstable OSL component was found. This component causes significant age underestimates as a larger proportion of the total signal is integrated. This effect can be avoided by using the initial channel of the OSL signal when calculating the equivalent dose.

The pattern of sensitivity change during an SAR measurement sequence was found to be dependent on sample age, preheat temperature and regeneration dose. These observations may be explained in terms of dose quenching and thermal activation. In certain circumstances, the 110°C thermoluminescence signal is not an appropriate proxy for OSL sensitivity. The SAR sensitivity correction was found to be appropriate irrespective of the sensitivity changes observed.

Several different patterns of equivalent dose distributions were found for the samples dated, ranging from limited, to considerable scatter. Possible causes for this scatter are discussed

Samples from the Inhaca and Bazaruto Islands were dated using the SAR technique. These islands are composed of large dunes, which were dated in an

attempt to understand the evolution of each island, in relationship to sea-level change. On both islands, the main sedimentary units were deposited during previous interglacials (high sea-level). However, some localised remobilisation of these dunes occurred during the Last Glacial Maximum, possibly in response to lowered regional water tables, due to low sea-levels. Significant aeolian activity is also recorded during the Holocene.

Bibliography

(from 1st October 2002 to 31st March 2003) Compiled by Ann Wintle

---

Bailiff, I. K. and Mikhailik, V. B. (2003). Spatially-resolved measurement of optically stimulated luminescence and time-resolved luminescence. *Radiation Measurements* **37**, 151-159.

Bartoll, J., Schwarcz, H. P. and Rink, W. J. (2002). ESR of E' centres in unstrained geological quartz grains. *Applied Radiation and Isotopes* **57**, 491-496.

Benn, D. I. and Owen, L. A. (2002). Himalayan glacial sedimentary environments: a framework for reconstructing and dating the former extent of glaciers in high mountains. *Quaternary International* **97-8**, 3-25.

Callens, F., Vanhaelewyn, G. and Matthys, P. (2002). Some recent multi-frequency electron paramagnetic resonance results on systems relevant for dosimetry and dating. *Spectrochimica Acta A* **58**, 1321-1328.

Carneiro, A., Schwartz, D., Tatumi, S. H. and Rosique, T. (2002). Amazonian paleodunes provide evidence for drier climate phases during the Late Pleistocene-Holocene. *Quaternary Research* **58**, 205-209.

Chithambo, M. L. (2003). Dependence of the thermal influence on luminescence lifetimes from quartz on the duration of optical stimulation. *Radiation Measurements* **37**, 167-175.

Choi, J. H., Murray, A. S., Jain, M., Cheong, C. S. and Chang, H. W. (2003). Luminescence dating of well-sorted marine terrace sediments on the southeastern coast of Korea. *Quaternary Science Reviews* **22**, 407-421.

Dos Santos, L. H. E. and Watanabe, S. (2002). Effects of pre-irradiation on EPR, optical absorption and TL of albite. *Radiation Effects and Defects in Solids* **157**, 743-749.

Duller, G. A. T. (2003). Distinguishing quartz and feldspar in single grain luminescence measurements. *Radiation Measurements* **37**, 161-165.

Dutkiewicz, A., Von der Borch, C. C. and Prescott, J. R. (2002). Geomorphology of the Lake Malata-Lake Greenly complex, South Australia, and its implications for Late Quaternary palaeoclimate. *Transactions of the Royal Society of South Australia* **126**, 103-115.

Formento-Trigilio, M. L., Burbank, D. W., Nicol, A., Shulmeister, J. and Rieser, U. (2003). River response to an active fold-and-thrust belt in a convergent margin setting, North Island, New Zealand. *Geomorphology* **49**, 125-152.

Galloway, R. B. (2002). Comparison of luminescence lifetimes in quartz following alpha and beta irradiations. *Radiation Measurements* **35**, 591-593.

Galloway, R. B. (2003). Limestone: some observations on luminescence in the region of 360 nm. *Radiation Measurements* **37**, 177-185.

Habermann, A. (2002). Quantitative cathodoluminescence (CL) spectroscopy of minerals: possibilities and limitations. *Mineralogy and Petrology* **76**, 247-259.

Hoffmann, D., Woda, C. and Mangini, A. (2003). Equivalent dose determination in foraminifera: analytical description of the CO2 signal dose-response curve. *Radiation Measurements* **37**, 95-101.

Itoh, N., Stoneham, D. and Stoneham, A. M. (2002). Ionic and electronic processes in quartz: mechanisms of thermoluminescence and optically stimulated luminescence. *Journal of Applied Physics* **92**, 5036-5044.

Ivliev, A. I., Badyukov, D. D., Kuyunko, N. S. and Kozlov, E. A. (2002). A study of thermoluminescence in experimentally shocked samples. III: Calcite. *Geochemistry International* **40**, 739-750.

Jain, M., Bøtter-Jensen, L. and Singhvi, A. K. (2003). Dose evaluation using multiple-aliquot quartz OSL: test of methods and a new protocol for improved accuracy and precision. *Radiation Measurements* **37**, 67-80.

Jakobsson, M., Backman, J., Murray, A. and Lovlie, R. (2003). Optically stimulated luminescence dating supports central Arctic Ocean cm-scale sedimentation rates. *Geochemistry Geophysics Geosystems* **4**, art no 1016.

Kalchgruber, R., Göksu, H. Y., Hochhauser, E. and Wagner, G. A. (2002). Monitoring environmental dose rate using Risø TL/OSL readers with built-in sources: recommendations for users. *Radiation Measurements* **35**, 585-590.

Kendrick, K. J., Morton, D. M., Wells, S. G. and Simpson, R. W. (2002). Spatial and temporal deformation along the northern San Jacinto fault, northern California: implications for slip rates. *Bulletin of the Seismological Society of America* **92**, 2782-2802.

Kinoshita, A., Brunetti, A., Avelar, W. E. P., Mantelatto, F. L. M., Simoes, M. G., Fransozo, A. and Baffa, O. (2002). ESR dating of a subfossil shell from Couve Island, Ubatuba, Brazil. *Applied Radiation and Isotopes* **57**, 497-500.

Kitis, G., Liritzis, I. and Vafeiadou, A. (2002). Deconvolution of optical stimulated luminescence decay curves. *Journal of Radioanalytical and Nuclear Chemistry* **254**, 143-149.

Kjaer, K. H., Demidov, I. N., Larsen, E., Murray, A. and Nielsen, J. K. (2003). Mezen Bay - a key area for understanding Weichselian glaciations in northern Russia. *Journal of Quaternary Science* **18**, 73-93.

Koike, C., Chihara, H., Koikie, K., Nakagawa, M., Okada, M., Tsuchiyama, A., Aoki, M., Awata, T. and Atobe, K. (2002). Thermoluminescence of forsterite and fused quartz as a candidate for the extended red emission. *Meteoritics and Planetary Science* **37**, 1591-1598.

Krbetschek, M. R., Götze, J., Irmer, G., Rieser, U. and Trautmann, T. (2002). The red luminescence emission of feldspar and its wavelength dependence on K, Na, Ca-composition. *Mineralogy and Petrology* **76**, 167-177.

Lancaster, N., Kocurek, G., Singhvi, A. K., Pandey, V., Deynoux, M., Ghienne, J.-F. and Lo, K. (2002). Late Pleistocene and Holocene dune activity and wind regimes in the western Sahara Desert of Mauritania. *Geology* **30**, 991-994.

Laukhin, S. A., Ronen, A., Pospelova, G. A., Sharonova, Z. V., Ranov, V. A., Burukeiewicz, J. M., Volgina, V. A. and Tsatskin, A. (2001). New data on the geology and geochronology of the Lower Palaeolithic site Bizat Ruhama in the southern Levant. *Paléorient* **27**, 69-80.

Laukhin, S. A., Ronen, A., Ranov, V. A., Pospelova, G. A., Burdukevich, Y. M., Sharonova, Z. V., Volgina, V. A., Kulikov, O. A., Vlasov, V. K. and Tsatskin, A. (2000). New data on the Paleolithic geochronology in southern Levant. *Stratigraphy and Geological Correlation* **8**, 598-510.

Maher, B. A., Hu, M. Y., Roberts, H. M. and Wintle, A. G. (2003). Holocene loess accumulation and soil development at the western edge of the Chinese Loess Plateau: implication for magnetic proxies of palaeorainfall. *Quaternary Science Reviews* **22**, 445-451.

Marsh, R. E., Prestwich, W. V., Rink, W. J. and Brennan, B. J. (2002). Monte Carlo determinations of the beta dose rate to tooth enamel. *Radiation Measurements* **35**, 609-616.

Misdaq, M. A., Oufni, L., Erramli, H., Boudad, L. and Kabiri, L. (2002). Dating of a Quaternary limestone cave by combining the SSNTD technique with paleodose measurements: application to the stalagmite and stalagmite growth. *Radiation Measurements* **35**, 339-345.

Molodkov, A. N. and Bolikhovskaya, N. S. (2002). Eustatic sea -level and climate change over the last 600 ka as derived from mollusc-based ESR-chronostratigraphy and pollen evidence in Northern Eurasia. *Sedimentary Geology* **150**, 185-201.

Moumani, K., Alexander, J. and Bateman, M. D. (2003). Sedimentology of the Late Quaternary Wadi Hasa Marl Formation of Central Jordan: a record of climate variability. *Palaeogeography, Palaeoclimatology, Palaeoecology* **191**, 221-242.

Nichol, S. L., Lian, O. B. and Carter, C. H. (2003). Sheet-gravel evidence for a late Holocene tsunami run-up on beach dunes, Great Barrier Island, New Zealand. *Sedimentary Geology* **155**, 129-145.

Orford, J. D., Murdy, J. M. and Wintle, A. G. (2003). Prograded Holocene beach ridges with superimposed dunes in north-east Ireland: mechanisms and timescales of fine and coarse beach sediment decoupling and deposition. *Marine Geology* **194**, 47-64.

Owen, L. A., Kamp, U., Spencer, J. Q. and Haserodt, K. (2002). Timing and style of Late Quaternary glaciation in the eastern Hindu Kush, Chitral, northern Pakistan: a review and revision of the glacial chronology based on new optically stimulated luminescence dating. *Quaternary International* **97-8**, 41-55.

Pack, S. M., Miller, G. H., Fogel, M. L. and Spooner, N. A. (2003). Carbon isotopic evidence for increased aridity in northwestern Australia through the Quaternary. *Quaternary Science Reviews* **22**, 629-643.

Paddaya, K., Blackwell, B. A. B., Jhaldiyal, R., Petraglia, M. D., Fevrier, S., Chaderton, D. A., Blickstein, J. I. B. and Skinner, A. R. (2002). Recent findings on the Acheulian of the Hunsgi and Baichbal valleys, Karnataka, with special reference to the Isampur excavation and its dating. *Current Science* **83**, 641-647.

Polikreti, K., Michael, C. T. and Maniatis, Y. (2003). Thermoluminescence characteristics of marble and dating of freshly excavated marble objects. *Radiation Measurements* **37**, 87-94.

Prentice, C. S., Kendrick, K., Berryman, K., Bayasgalan, A., Ritz, J. F. and Spencer, J. Q. (2002). Prehistoric ruptures of the Gurvan Bulag fault, Gobi Altay, Mongolia. *Journal of Geophysical Research - Solid Earth* **107**, art no 2321.

Rao, T. K. G., Rajendran, C. P., Mathew, G. and John, B. (2002). Electron spin resonance dating of fault gouge from Desamangalam, Kerala: evidence for Quaternary movement in Palghat gap shear zone. *Proceedings of the Indian Academy of Sciences - Earth and Planetary Sciences* **111**, 103-113.

Rawling, J. E., Fredlund, G. G. and Mahan, S. (2003). Aeolian cliff-top deposits and buried soils in the White River badlands, South Dakota, USA. *The Holocene* **13**, 121-129.

Ree, J. H., Lee, Y. J., Rhodes, E. J., Park, Y., Kwon, S. T., Chwae, U., Jeon, J. S. and Lee, B. (2003). Quaternary reactivation of tertiary faults in the southeastern Korean Peninsula: age constraint by optically stimulated luminescence dating. *Island Arc* **12**, 1-12.

Regnauld, H., Mauz, B. and Morzadec-Kerfourn, M. T. (2003). The last interglacial shoreline in northern Brittany, western France. *Marine Geology* **194**, 65-77.

Rink, W. J., Kandel, A. W. and Conard, N. J. (2002). The ESR geochronology and geology of the open-air Palaeolithic deposits in Bollschweil, Germany. *Archaeometry* **44**, 635-650.

Rink, W. J., Richter, D., Schwarcz, H. P., Marks, M. E., Monigal, K. and Kaufman, D. (2003). Age of the Middle Palaeolithic site of Rosh Ein Mor, Central Negev, Israel; Implications for the age range of the early Levantine Mousterian of the Levantine corridor. *Journal of Archaeological Science* **30**, 195-204.

Roque, C., Guibert, P., Vartanian, E., Bechtel, F., Treuil, R., Darcque, P., Koukoli-Chryssanthaki, H. and Malamidou, D. (2002). The chronology of the Neolithic sequence at Dikili Tash, Macedonia, Greece: TL dating of domestic ovens. *Archaeometry* **44**, 613-633.

Schnepp, E., Pucher, R., Goedicke, C., Manzano, A., Müller, U. and Lanos, P. (2003). Paleomagnetic directions and thermoluminescence dating from a bread oven-floor sequence in Lübeck (Germany): a record of 450 years of geomagnetic secular variation. *Journal of Geophysical Research* **108**.

Soliman, C. and Hussein, M. A. (2002). Sensitization of the first thermoluminescence peak in natural orthoclase. *Japanese Journal of Applied Physics* **41**, 6184-6188.

Sunta, C. M., Ayta, W. E. F., Chubaci, J. F. D. and Watanabe, S. (2002). Test for quasi-equilibrium in thermally stimulated luminescence and conductivity. *Radiation Measurements* **35**, 595-602.

Thompson, S. C., Weldon, R. J., Rubin, C. M., Abdrakhmatov, K., Molnar, P. and Berger, G. W. (2002). Late Quaternary slip rates across the central Tien Shan, Kyrgyzstan, central Asia. *Journal of Geophysical Research - Solid Earth* **107**, art. no. 2203.

Thorp, M., Glanville, P., Stokes, S. and Bailey, R. (2002). Preliminary optical and radiocarbon determinations for Upper Pleistocene alluvial sediments in the southern Anti Atlas Mountains, Morocco. *Comptes Rendus Geoscience* **334**, 903-908.

Törnqvist, T. E., Wallinga, J. and Busschers, F. S. (2003). Timing of the last sequence boundary in a fluvial setting near the highstand shoreline - insights from optical dating. *Geology* **31**, 279-282.

Tsukamoto, S., Asahi, K., Watanabe, T. and Rink, W. J. (2002). Timing of past glaciations in Kanchenjunga Himal, Nepal by optically stimulated luminescence dating of tills. *Quaternary International* **97-8**, 57-67.

Turkin, A. A., van Es, H. J., Vainshtein, D. I. and den Hartog, H. W. (2002). Protocol for TL dating with zircon: computer simulation of temperature and dose rate effects. *Radiation Effects and Defects in Solids* **157**, 833-838.

van Es, H. J., Vainshtein, D. I., de Meijer, R. J., den Hartog, H. W., Donoghue, J. F. and Rozendaal, A. (2002). Mineral zircon: a novel thermoluminescence geochronometer. *Radiation Effects and Defects in Solids* **157**, 1063-1070.

Wallinga, J. (2002). Optically stimulated luminescence dating of fluvial deposits: a review. *Boreas* **31**, 303-322.

Watanabe, S., Feria Ayta, W. E., Hamaguchi, H., Guidon, N., La Salvia, E. S., Maranca, S. and Filho, O. B. (2003). Some evidence of a date of first humans to arrive in Brazil. *Journal of Archaeological Science* **30**, 351-354.

Waychunas, G. A. (2002). Apatite luminescence. *Reviews in Mineralogy and Geochemistry* **48**, 701-742.

Wolfe, S. A., Ollerhead, J., Huntley, D. J. and Campbell, C. (2002). Late Holocene dune activity in the Duchess dune field, Alberta. *Geological Survey of Canada, Current Research* **B3**, 1-8.

Wrinne, P. J. and Rink, W. J. (2003). ESR dating of tooth enamel from Aterian levels at Mugharet el 'Aliya (Morocco). *Journal of Archaeological Science* **30**, 123-133.

Xing, C. Q., Yin, G. M., Ding, G. Y., Lu, Y. C., Shen, X. H., Tian, Q. J., Chai, Z. H. and Wei, K. B. (2002). Thickness of calcium carbonate coats on stones of the Heishanxia terraces of the Yellow River and dating of coarse elastic sedimentary geomorphic surfaces. *Chinese Science Bulletin* **47**, 1594-1600.

Yada, T., Norizawa, K., Hirai, M., Yamanaka, C. and Ikeya, M. (2002). Optically stimulated luminescence study on gamma-irradiated ice frozen from H2O and D2O. *Japanese Journal of Applied Physics Part 1* **41**, 5874-5880.

Yi, C. L., Jiao, K. Q., Liu, K. X., He, Y. Q. and Ye, Y. G. (2002). ESR dating of the sediments of the Last Glaciation at the source area of the Urumqi River, Tian Shan Mountains, China. *Quaternary International* **97-8**, 141-146.

Yin, G. M., Zhao, H., Yin, J. H. and Lu, Y. C. (2002). Chronology of the stratum containing the skull of the Dali Man. *Chinese Science Bulletin* **47**, 1302-1307.

Zdravkova, M., Denis, J.-M., Gallez, B. and Debuyst, R. (2002). Sensitivity of whole human teeth to fast neutrons and gamma-rays estimated by L-band EPR spectroscopy. *Radiation Measurements* **35**, 603-608.

Zheng, H. B., Powell, C. M. A. and Zhao, H. (2003). Eolian and lacustrine evidence of late Quaternary palaeoenvironmental changes in southwestern Australia. *Global and Planetary Change* **35**, 75-92.

Zhou, S. Z., Jiao, K. Q., Zhao, J. D., Zhang, S. Q., Cui, J. X. and Xu, L. B. (2002). Geomorphology of the Urumqui River Valley and the uplift of the Tianshan Mountains in Quaternary. *Science in China Series D* **45**, 961-.

Zhou, S. Z., Li, J. J. and Zhang, S. Q. (2002). Quaternary glaciation of the Bailang River Valley, Qilian Shan. *Quaternary International* **97-8**, 103-110.